



CKM 2016

9<sup>th</sup> International Workshop on the CKM Unitarity Triangle

28<sup>th</sup> November - 2<sup>nd</sup> December 2016

Tata Institute of Fundamental Research, Mumbai

## Latest ATLAS Results on $\phi_s$

Pavel Řezníček (*Charles University, Prague*), on behalf of the ATLAS collaboration





# The ATLAS Experiment

General purpose detector

## Calorimeter System

EM and Hadronic energy

- LAr EM barrel and EC
- LAr Had. EC
- Tile Calorimeter (Fe-Scin.) hadronic barrel

## Muon Spectrometer

Toroid Magnets

Precision  $\mu$  tracking:

- MDT (Monitored Drift Tubes)
- CSC (Cathode Strip Chambers)

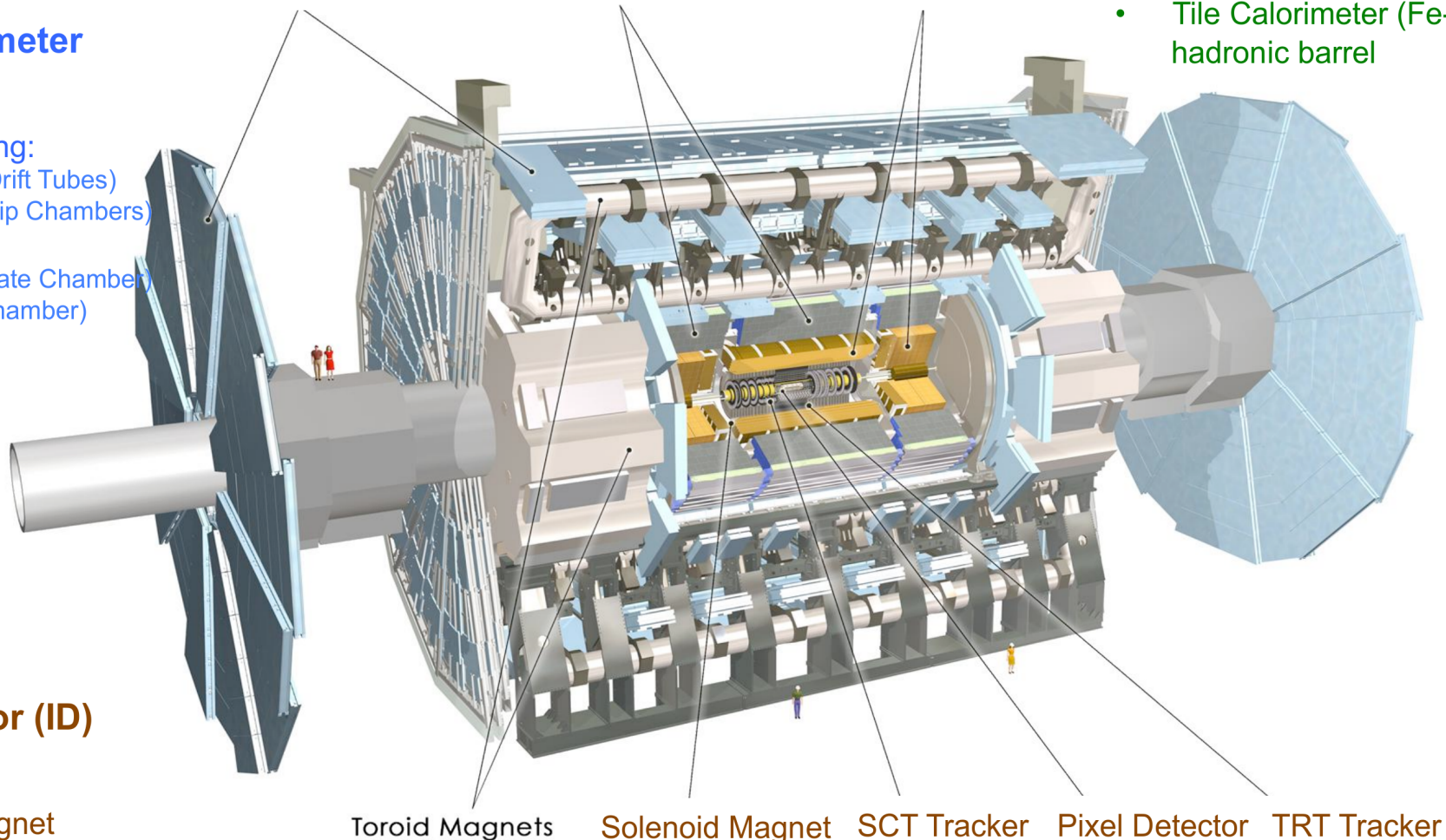
Trigger:

- RPC (Resistive Plate Chamber)
- TGC (Thin Gas Chamber)

Muon detectors

Tile Calorimeter

Liquid Argon Calorimeter



## Inner Detector (ID)

Tracking

2T Solenoid Magnet

- Silicon Pixels,  $50 \times 400 \mu\text{m}^2$
- Silicon Strips (SCT),  $80 \mu\text{m}$  stereo
- Transition Radiation Tracker (TRT) 36 points/track

Toroid Magnets

Solenoid Magnet

SCT Tracker

Pixel Detector

TRT Tracker



# The ATLAS Experiment

- Triggering  $|\eta| < 2.4$
- Precision Tracking  $|\eta| < 2.7$

## Muon Spectrometer

Toroid Magnets

Precision  $\mu$  tracking:

- MDT (Monitored Drift Tubes)
- CSC (Cathode Strip Chambers)

Trigger:

- RPC (Resistive Plate Chamber)
- TGC (Thin Gas Chamber)

Muon detectors

## B-Physics

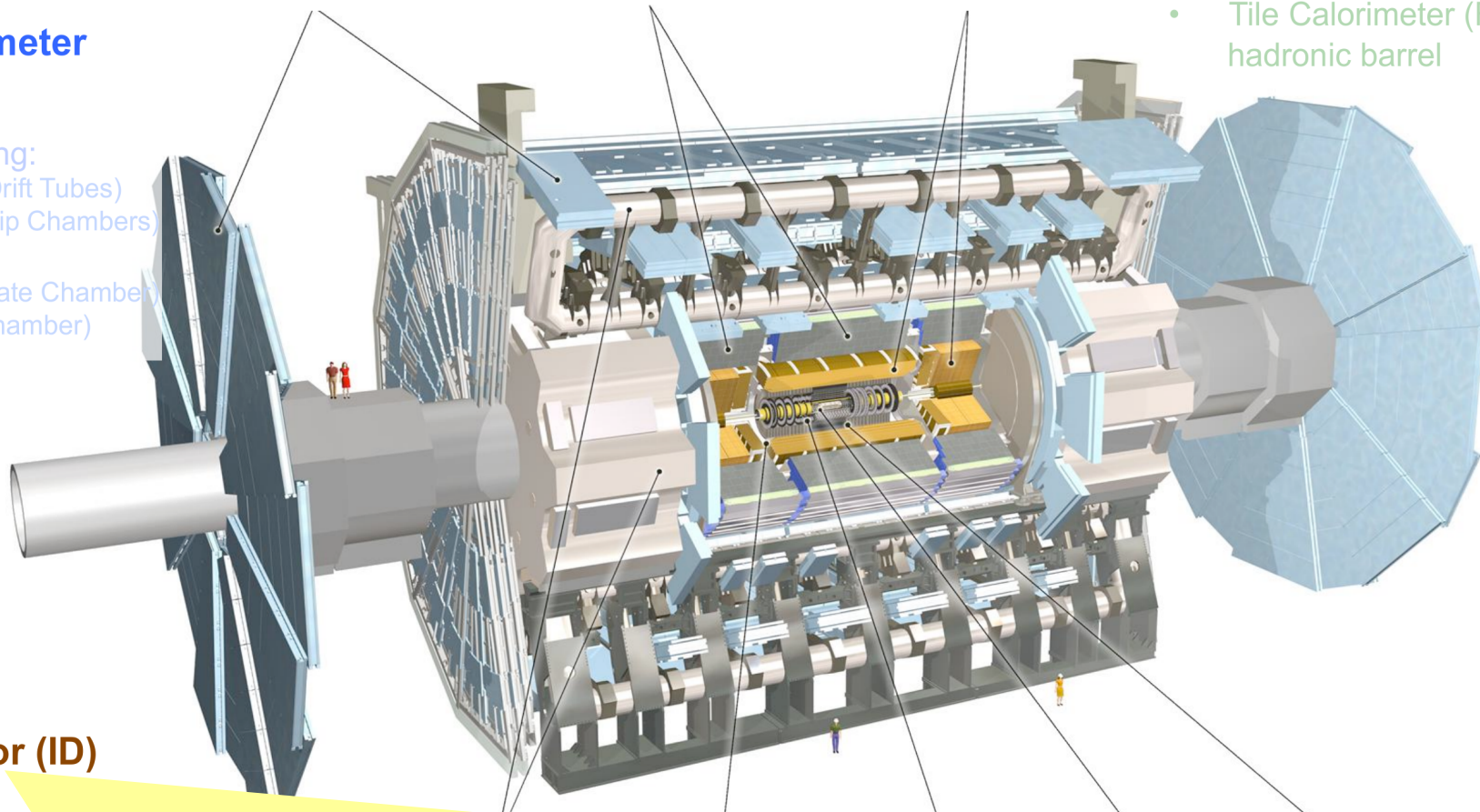
Tile Calorimeter

Liquid Argon Calorimeter

## Calorimeter System

EM and Hadronic energy

- LAr EM barrel and EC
- LAr Had. EC
- Tile Calorimeter (Fe-Scin.) hadronic barrel



## Inner Detector (ID)

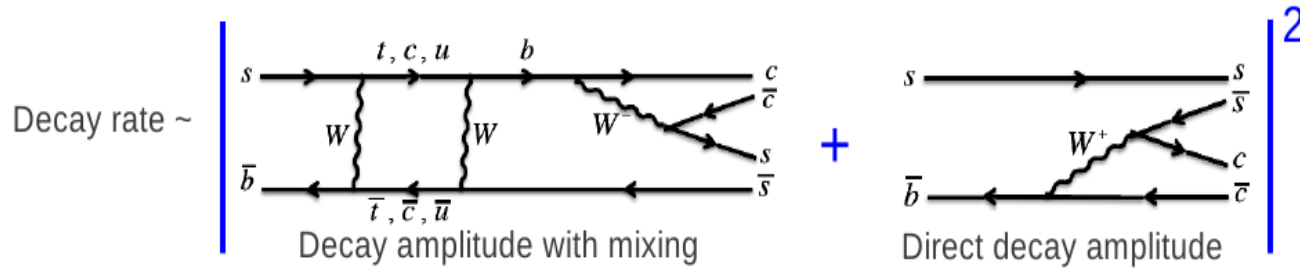
- $p_T > 0.4$  GeV,  $|\eta| < 2.5$
- **New for Run2: Insertable B-Layer (IBL)** an additional inner-most pixel layer ( $r = 33$ mm) and lower  $x/X_0$  beam pipe

- Resolution in  $m_{\mu+\mu-}$ : around 50 MeV for  $J/\psi$  and 150 MeV for  $\Upsilon(nS)$
- Resolution in b-hadron proper decay time in Run-1 data around 100 fs (~30% improvement with IBL in Run-2)



# Measurement of $\Delta\Gamma_s$ and $\phi_s$ in $B_s \rightarrow J/\psi(\mu\mu)\phi(KK)$

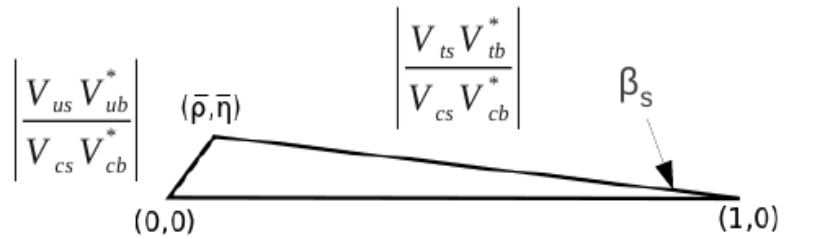
- CP violation in  $B_s \rightarrow J/\psi\phi$  occurs through the interference in mixing and decay



- $B_s$  mixing:**
- Mass difference  $\Delta m = m_H - m_L$
  - Mixing phase  $\phi_s$
  - Decay width difference  $\Delta\Gamma_s = \Gamma_L - \Gamma_H$
- $$\begin{aligned} |B_s^H\rangle &= p|B_s^0\rangle - q|B_s^{\bar{0}}\rangle \\ |B_s^L\rangle &= p|B_s^0\rangle + q|B_s^{\bar{0}}\rangle \end{aligned}$$

- Time evolution of flavour tagged  $B_s \rightarrow J/\psi\phi$  very sensitive to New Physics
- 9 physics parameters to describe  $B_s \rightarrow J/\psi\phi$  decay

- $\Gamma_s, \Delta\Gamma_s$  decay with and decay width difference
- $\phi_s (\approx 2\beta_s)$  CP violating phase
- $|A_0|^2, |A_{||}|^2$  CP state amplitudes
- $\delta_{||}, \delta_{\perp}$  Strong phases
- $|A_S|^2, \delta_S$  S-wave parameters



$\phi_s$  small in SM, clear to see potential excess from NP

Measurement:

$$\frac{d^4\Gamma}{dt d\Omega} = \sum_{k=1}^{10} \mathcal{O}^{(k)}(t) g^{(k)}(\theta_T, \psi_T, \phi_T)$$



# Datasets and Selection

- Latest result using Run-1 pp collision data at 8 TeV, combined with previous 7 TeV analysis

JHEP 1608 (2016) 147

PRD 90 (2014) 052007

- **Datasets (pp):** 7 TeV data, 5.08 fb<sup>-1</sup> (used 4.9 fb<sup>-1</sup>), L<sub>max</sub> = 3.7×10<sup>33</sup> cm<sup>-2</sup>s<sup>-1</sup>  
8 TeV data, 21.3 fb<sup>-1</sup> (used 14.3 fb<sup>-1</sup>), L<sub>max</sub> = 7.7×10<sup>33</sup> cm<sup>-2</sup>s<sup>-1</sup>

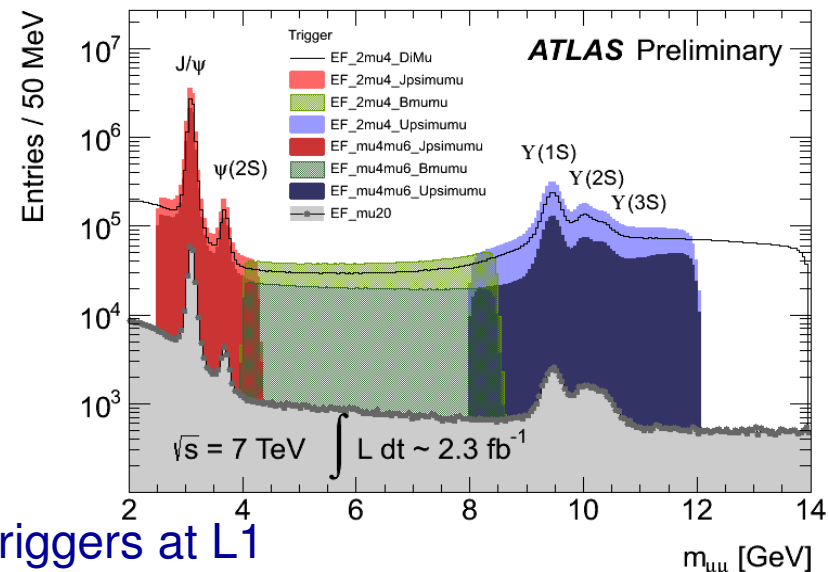
- **Trigger:** 20 MHz collision rate → ~400 Hz recording

- B-physics concentrates on low-p<sub>T</sub> di-muon signatures, in this case J/ψ → μμ

- Trigger on low-p<sub>T</sub> (4,6 GeV) di-muon

- 2 muons at L1 (HW-based)
- Confirmed at HLT
- Track vertex fit and J/ψ mass cuts at HLT

- 8 TeV data: low-p<sub>T</sub> maintained introducing barrel triggers at L1



- **Selection:** full B<sub>s</sub> → J/ψ(μ<sup>+</sup>μ<sup>-</sup>)φ(K<sup>+</sup>K<sup>-</sup>) decay chain reconstruction with Inner Detector, no K/π separation

- J/ψ selection – di-muon vertex  $\chi^2/\text{NDF} < 10$ , J/ψ invariant mass windows width 0.27 ... 0.48 GeV (barrel → endcap)

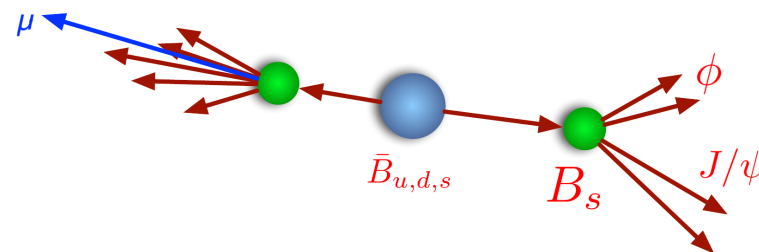
- φ selection – p<sub>T</sub>(K<sup>±</sup>) > 1 GeV, φ invariant mass window 22 MeV

- B<sub>s</sub> candidates – 4-track vertex  $\chi^2/\text{NDF} < 3$ , J/ψφ invariant mass range for analysis (5.15 – 5.65) GeV, no proper decay time cut



# B-Flavour Tagging in $B_s \rightarrow J/\psi \phi$

- Knowledge of  $B_s/\bar{B}_s$  flavour at production significantly increases signal PDF sensitivity to  $\phi_s$
- Three taggers: muon, electron, b-tagged jet
- Key variable: charge of  $p_T$ -weighted tracks in a cone ( $\Delta R$ ) around the opposite side primary object ( $\mu, e, b$ -jet), used to build per-candidates  $B_s$  tag probability



**Muon tagger:**

- muon  $p_T > 2.5$  GeV
- $\Delta z(\mu)$  w.r.t. PV  $< 5$  mm
- $\Delta R$  (cone) = 0.5
- $\kappa = 1.1$
- tracks  $p_{Ti} > 0.5$  GeV

**Electron tagger:**

- electron  $p_T > 0.5$  GeV
- $\Delta z(e)$  w.r.t. PV  $< 5$  mm
- $\Delta R(e^\pm, B_s) > 0.4$
- $\Delta R$  (cone) = 0.5
- $\kappa = 1.0$
- tracks  $p_{Ti} > 0.5$  GeV

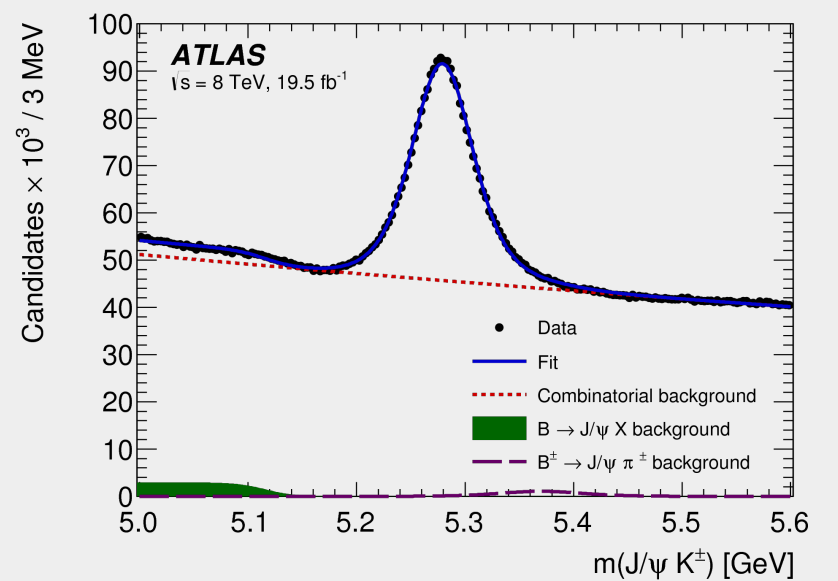
**b-jet tagger:**

- b-tag weight 0.7 maximizing the tagging power on  $B^\pm$  sample
- anti- $k_T$  ( $R = 0.8$ )
- $\kappa = 1.1$
- using all tracks associated to the jet

$$Q_{\text{jet}} = \frac{\sum_i^{N \text{ tracks}} q_i \cdot (p_{Ti})^\kappa}{\sum_i^{N \text{ tracks}} (p_{Ti})^\kappa}$$

$$Q_\mu = \frac{\sum_i^{N \text{ tracks}} q_i \cdot (p_{Ti})^\kappa}{\sum_i^{N \text{ tracks}} (p_{Ti})^\kappa}$$

- Calibration on self-tagged  $B^\pm \rightarrow J/\psi K^\pm$  channel: 3-track vertex,  $p_T(K) > 1$  GeV,  $L_{xy} > 0.1$  mm

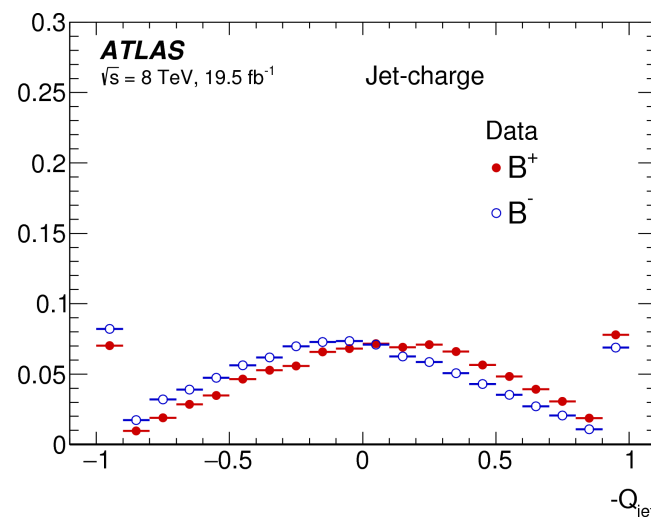
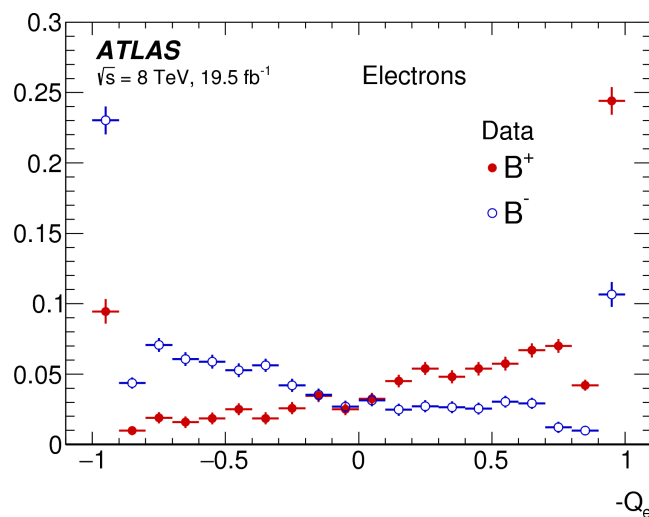
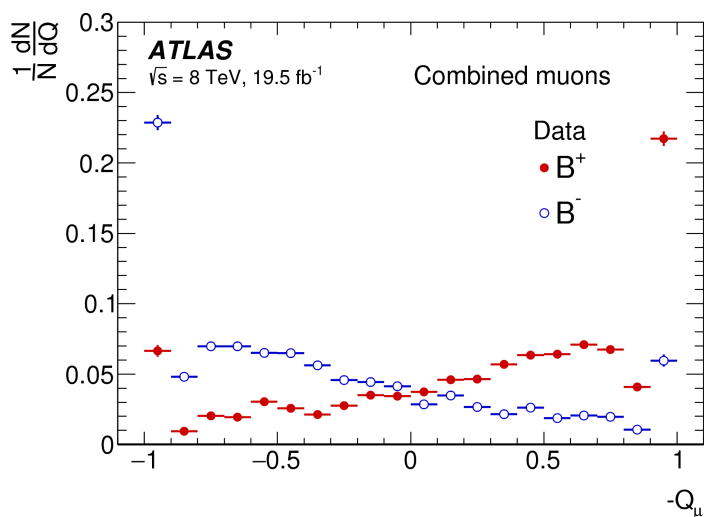




# B-Flavour Tagging Results

Tagger	Efficiency [%]	Dilution [%]	Tagging Power [%]
Combined $\mu$	$4.12 \pm 0.02$	$47.4 \pm 0.2$	$0.92 \pm 0.02$
Electron	$1.19 \pm 0.01$	$49.2 \pm 0.3$	$0.29 \pm 0.01$
Segment-tagged $\mu$	$1.20 \pm 0.01$	$28.6 \pm 0.2$	$0.10 \pm 0.01$
Jet-charge	$13.15 \pm 0.03$	$11.85 \pm 0.03$	$0.19 \pm 0.01$
Total	$19.66 \pm 0.04$	$27.56 \pm 0.06$	$1.49 \pm 0.02$

- Per each  $B_s$ -candidate, only one out of the available taggers is selected – the one with the highest Dilution





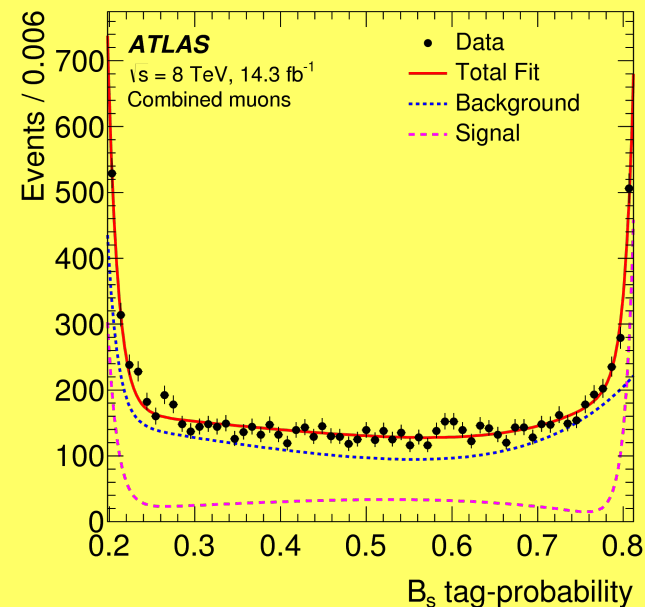
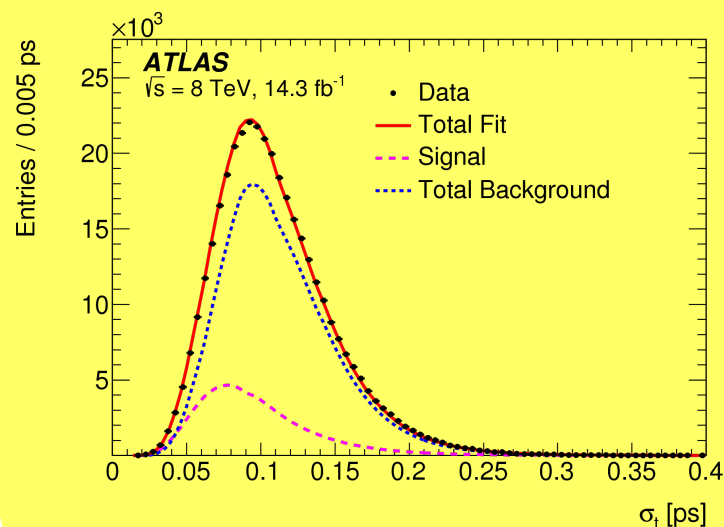
# Unbinned Maximum Likelihood Fit

$$\ln \mathcal{L} = \sum_{i=1}^N \left\{ w_i \cdot \ln \left( f_s \cdot \mathcal{F}_s(m_i, t_i, \sigma_{t_i}, \Omega_i, P(B|Q), p_{T_i}) \right. \right. \\ \left. \left. + f_s \cdot f_{B^0} \cdot \mathcal{F}_{B^0}(m_i, t_i, \sigma_{t_i}, \Omega_i, P(B|Q), p_{T_i}) \right. \right. \\ \left. \left. + f_s \cdot f_{\Lambda_b} \cdot \mathcal{F}_{\Lambda_b}(m_i, t_i, \sigma_{t_i}, \Omega_i, P(B|Q), p_{T_i}) \right. \right. \\ \left. \left. + (1 - f_s \cdot (1 + f_{B^0} + f_{\Lambda_b})) \mathcal{F}_{\text{bkg}}(m_i, t_i, \sigma_{t_i}, \Omega_i, P(B|Q), p_{T_i}) \right) \right\}$$

## Measured variables:

- $B_s$  mass  $m_i$
- $B_s$  proper decay time  $t_i$  and its uncertainty  $\sigma_{t_i}$
- 3 angles  $\Omega_i$  ( $\theta_{T_i}, \phi_{T_i}, \psi_{T_i}$ )
- $B_s$  momentum  $p_{T_i}$
- $B_s$  tag probability  $p_{B|Q_i}$
- tagging method  $M_i$

Signal and background PDFs for conditional observables determined from data using sidebands subtraction; PDFs fixed in the fit







# Unbinned Maximum Likelihood Fit

$$\ln \mathcal{L} = \sum_{i=1}^N \left\{ w_i \cdot \ln(f_s \cdot \mathcal{F}_s(m_i, t_i, \sigma_{t_i}, \Omega_i, P(B|Q), p_{T_i})) \right. \\
+ f_s \cdot f_{B^0} \cdot \mathcal{F}_{B^0}(m_i, t_i, \sigma_{t_i}, \Omega_i, P(B|Q), p_{T_i}) \\
+ f_s \cdot f_{\Lambda_b} \cdot \mathcal{F}_{\Lambda_b}(m_i, t_i, \sigma_{t_i}, \Omega_i, P(B|Q), p_{T_i}) \\
\left. + (1 - f_s \cdot (1 + f_{B^0} + f_{\Lambda_b})) \cdot \mathcal{F}_{\text{bkg}}(m_i, t_i, \sigma_{t_i}, \Omega_i, P(B|Q), p_{T_i}) \right\}$$

## Signal decay main parameters:

- CP violating phase  $\phi_s$
- Decay width  $\Gamma_s = (\Gamma_H + \Gamma_L)/2$
- Decay width difference  $\Delta\Gamma = \Gamma_H - \Gamma_L$
- CP state amplitudes  $|A_0(0)|^2$  and  $|A_{||}(0)|^2$
- Strong phases  $\delta_{||}$  and  $\delta_{\perp}$
- S-wave amplitude  $|A_S(0)|^2$  and phase  $\delta_S$  (fitting  $\delta_S - \delta_{\perp}$  to avoid high correlations)
- $B_s$  mean mass
- ( $\Delta m_s$  fixed to  $17.77 \text{ ps}^{-1}$ )

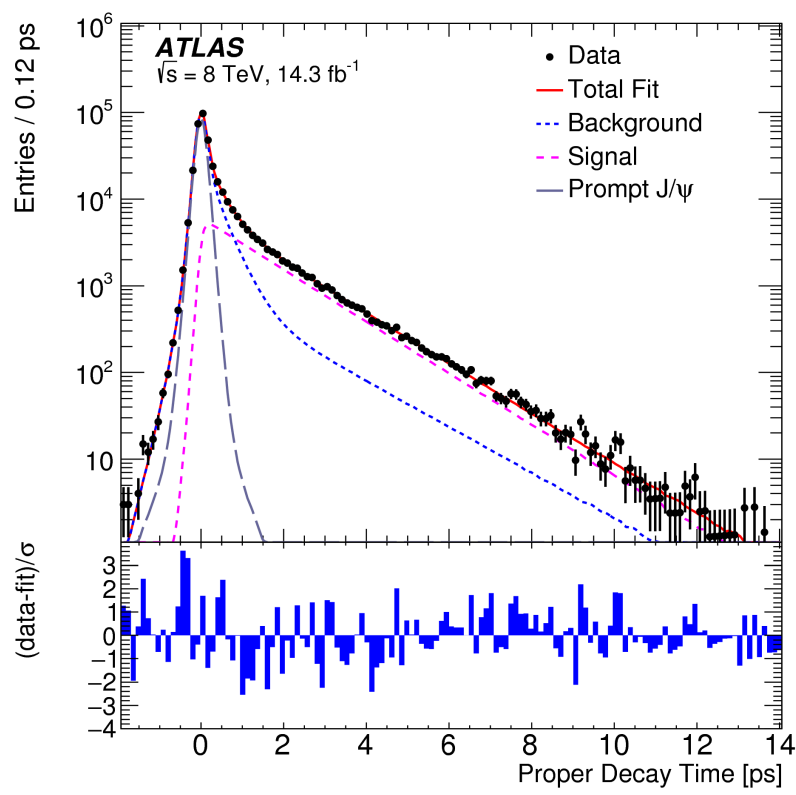
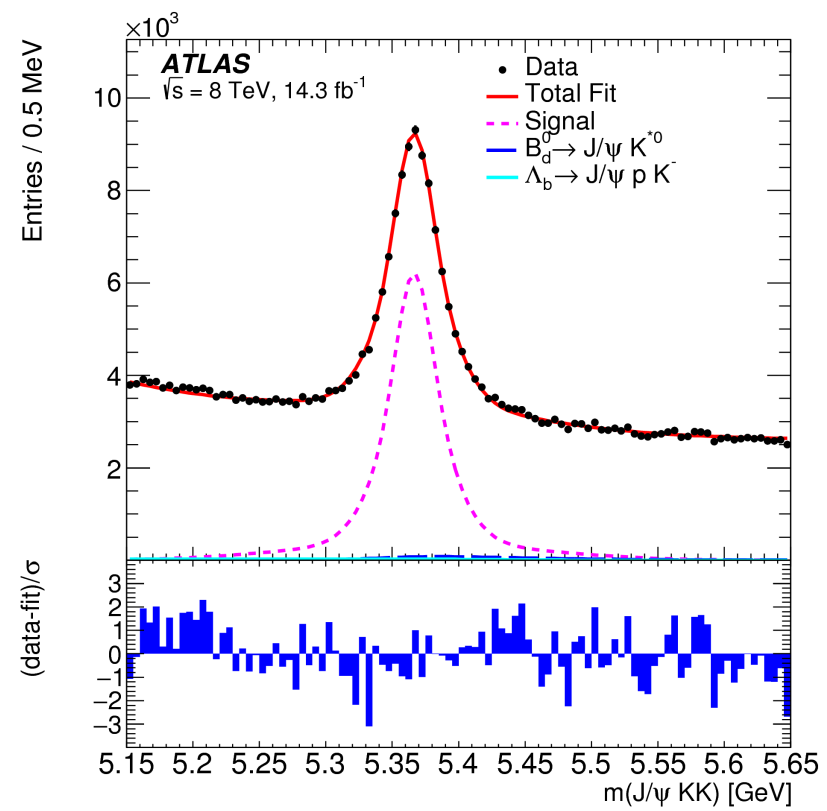
**$B_d \rightarrow J/\psi K^*(K\pi)$  and  $\Lambda_b \rightarrow J/\psi \Lambda^*(Kp)$  decay reflections**, derived from MC, PDG and the LHCb  $\Lambda_b \rightarrow J/\psi Kp$  measurement; fixed shape and relative contribution in the fit

**Combinatorial background** description, derived from data sidebands; angular distribution described by spherical harmonics and fixed in the fit

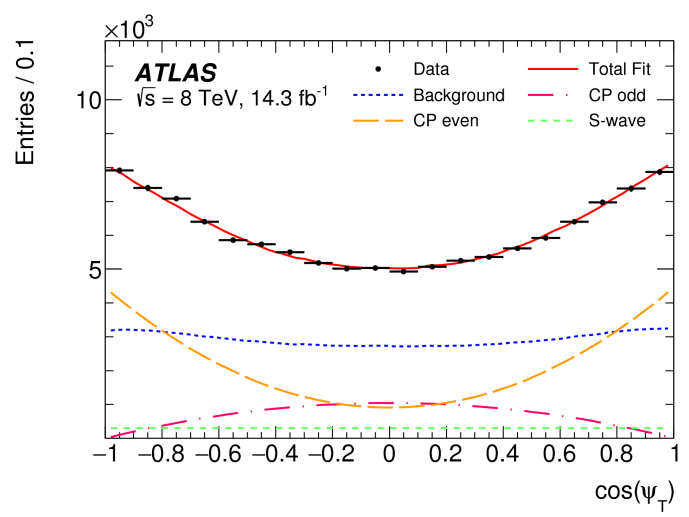
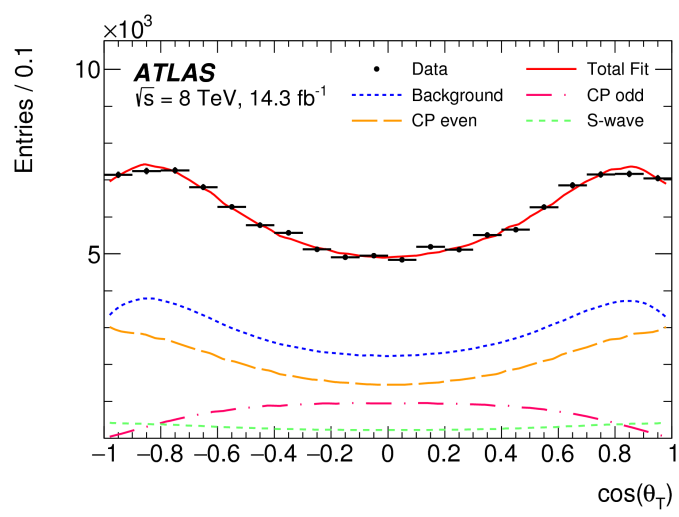
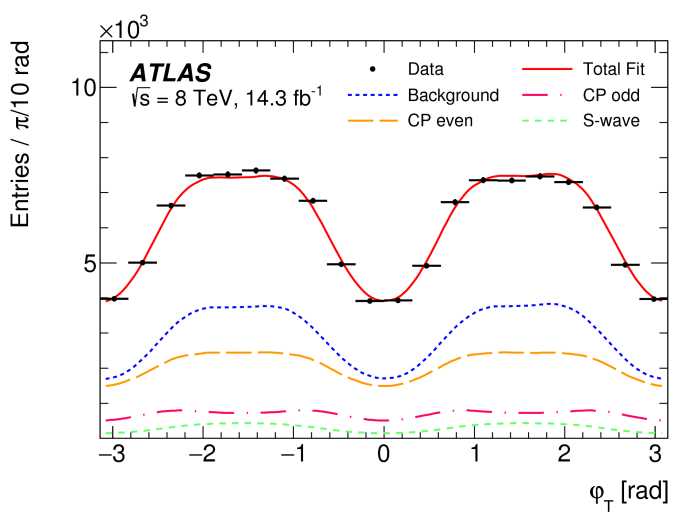
Weights accounting for **proper decay time trigger efficiency** (muons track  $d_0$  reconstruction efficiency bias); estimated from MC



# Fit Projections



$$\ln \mathcal{L} = \sum_{i=1}^N \{w_i \cdot \ln( f_s \cdot \mathcal{F}_s + f_s \cdot f_{B^0} \cdot \mathcal{F}_{B^0} + f_s \cdot f_{\Lambda_b} \cdot \mathcal{F}_{\Lambda_b} + (1 - f_{s, B^0, \Lambda_b}) \mathcal{F}_{\text{bkg}} )\}$$





# Systematic Uncertainties

	$\phi_s$ [rad]	$\Delta\Gamma_s$ [ps <sup>-1</sup> ]	$\Gamma_s$ [ps <sup>-1</sup> ]	$ A_{\parallel}(0) ^2$	$ A_0(0) ^2$	$ A_S(0) ^2$	$\delta_{\perp}$ [rad]	$\delta_{\parallel}$ [rad]	$\delta_{\perp} - \delta_S$ [rad]
■ Tagging	0.025	0.003	$<10^{-3}$	$<10^{-3}$	$<10^{-3}$	0.001	0.236	0.014	0.004
■ Acceptance	$<10^{-3}$	$<10^{-3}$	$<10^{-3}$	0.003	$<10^{-3}$	0.001	0.004	0.008	$<10^{-3}$
■ Inner detector alignment	0.005	$<10^{-3}$	0.002	$<10^{-3}$	$<10^{-3}$	$<10^{-3}$	0.134	0.007	$<10^{-3}$
■ Background angles model:									
Choice of $p_T$ bins	0.020	0.006	0.003	0.003	$<10^{-3}$	0.008	0.004	0.006	0.008
Choice of mass interval	0.008	0.001	0.001	$<10^{-3}$	$<10^{-3}$	0.002	0.021	0.005	0.003
■ $B_d^0$ background model	0.023	0.001	$<10^{-3}$	0.002	0.002	0.017	0.090	0.011	0.009
■ $\Lambda_b$ background model	0.011	0.002	0.001	0.001	0.007	0.009	0.045	0.006	0.007
■ Fit model:									
Mass signal model	0.004	$<10^{-3}$	$<10^{-3}$	0.002	$<10^{-3}$	0.001	0.015	0.017	$<10^{-3}$
Mass background model	$<10^{-3}$	0.002	$<10^{-3}$	0.002	$<10^{-3}$	0.002	0.027	0.038	$<10^{-3}$
Time resolution model	0.003	$<10^{-3}$	0.001	0.002	$<10^{-3}$	0.002	0.057	0.011	0.001
Default fit model	0.001	0.002	$<10^{-3}$	0.002	$<10^{-3}$	0.002	0.025	0.015	0.002
<b>Total</b>	0.042	0.007	0.004	0.006	0.007	0.022	0.30	0.05	0.01

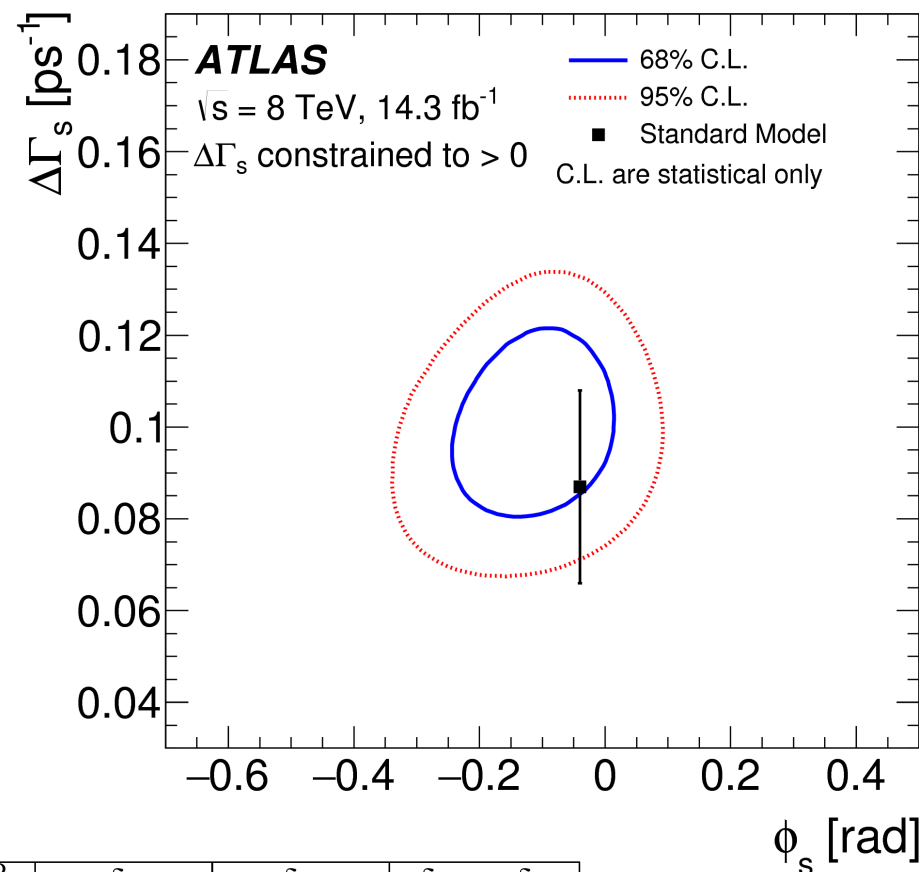
- Uncertainty in the calibration of the  $B_s$ -tag probability; MC statistical uncertainty included in fit stat. error
- Alternative detector acceptance fit-functions and binning determined from MC
- Radial expansion uncertainties determined from their effect on tracks  $d_0$  in the data
- Background angles model (fixed in UML fit) extracted from data with varying sidebands size and binning
- Uncertainties of relative fraction; fit-model and P-wave contribution
- Uncertainties of relative fraction; fit-model and contributions from  $\Lambda_b \rightarrow \Lambda^* J/\psi$  decays
- Toy-MC studies; pulls of the default fit model, default fit on toy-data generated with modified PDFs
- (Trigger efficiency modeling in MC found negligible)



# Result of the CPV $B_s \rightarrow J/\psi \phi$ Study

## Result with 8 TeV data

Parameter	Value	Statistical uncertainty	Systematic uncertainty
$\phi_s$ [rad]	-0.110	0.082	0.042
$\Delta\Gamma_s$ [ps <sup>-1</sup> ]	0.101	0.013	0.007
$\Gamma_s$ [ps <sup>-1</sup> ]	0.676	0.004	0.004
$ A_{  }(0) ^2$	0.230	0.005	0.006
$ A_0(0) ^2$	0.520	0.004	0.007
$ A_S(0) ^2$	0.097	0.008	0.022
$\delta_{\perp}$ [rad]	4.50	0.45	0.30
$\delta_{  }$ [rad]	3.15	0.10	0.05
$\delta_{\perp} - \delta_S$ [rad]	-0.08	0.03	0.01



## Fit correlation matrix:

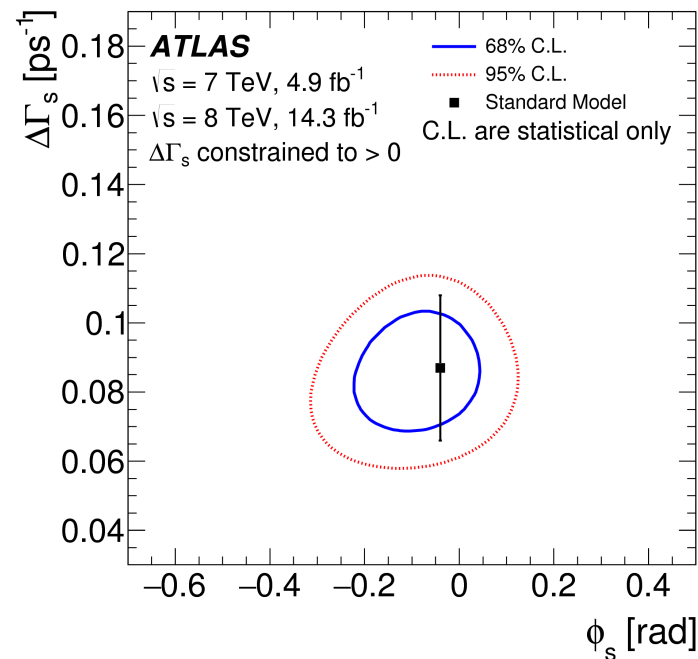
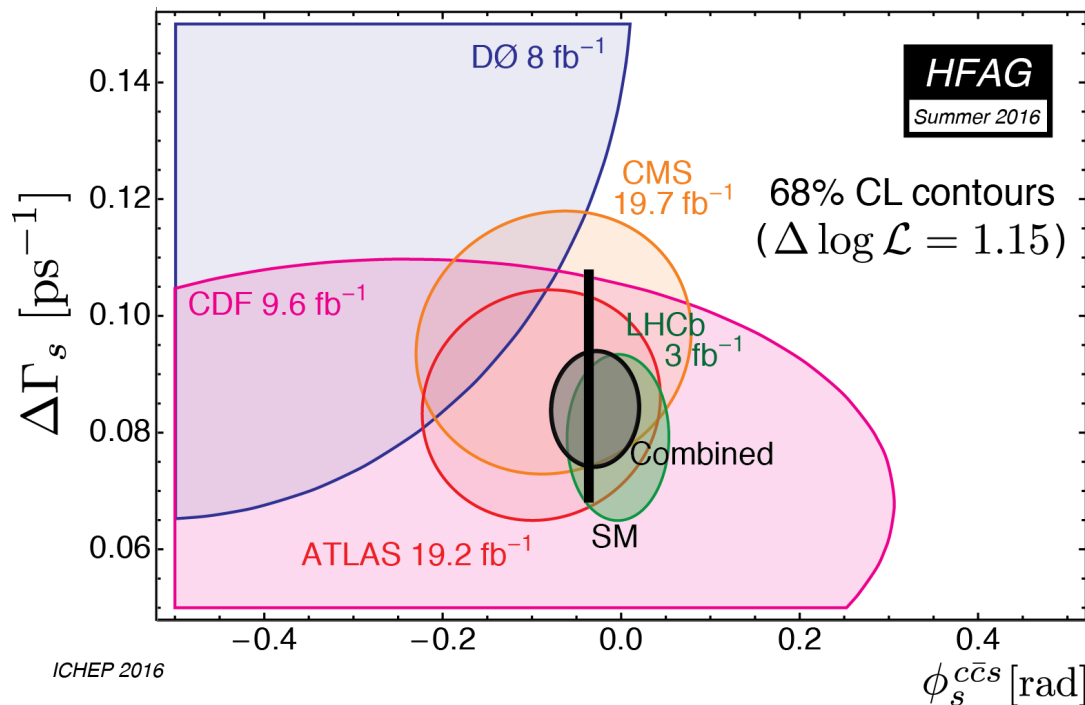
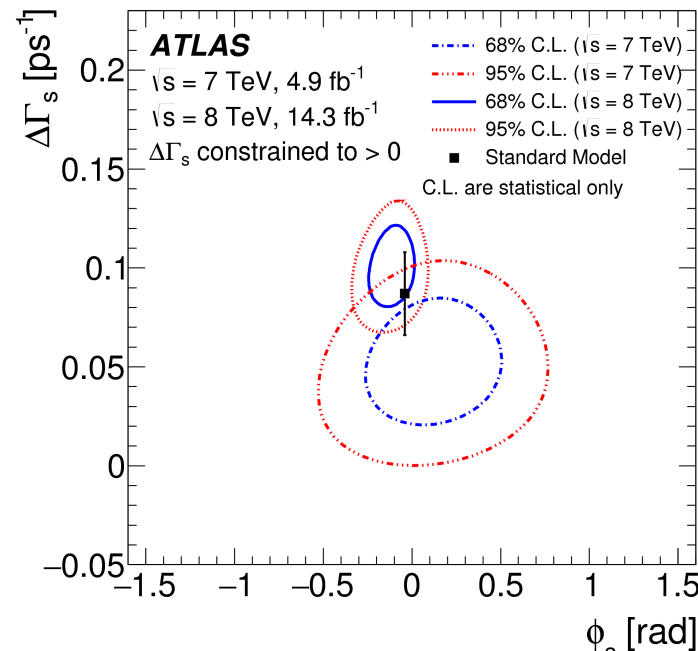
	$\Delta\Gamma$	$\Gamma_s$	$ A_{  }(0) ^2$	$ A_0(0) ^2$	$ A_S(0) ^2$	$\delta_{  }$	$\delta_{\perp}$	$\delta_{\perp} - \delta_S$
$\phi_s$	0.097	-0.085	0.030	0.029	0.048	0.067	0.035	-0.008
$\Delta\Gamma$	1	-0.414	0.098	0.136	0.045	0.009	0.008	-0.011
$\Gamma_s$		1	-0.119	-0.042	0.167	-0.027	-0.009	0.018
$ A_{  }(0) ^2$			1	-0.330	0.072	0.105	0.025	-0.018
$ A_0(0) ^2$				1	0.234	-0.011	0.007	0.014
$ A_S(0) ^2$					1	-0.046	0.004	0.052
$\delta_{  }$						1	0.158	-0.006
$\delta_{\perp}$							1	0.018



# Result of the CPV $B_s \rightarrow J/\psi \phi$ Study

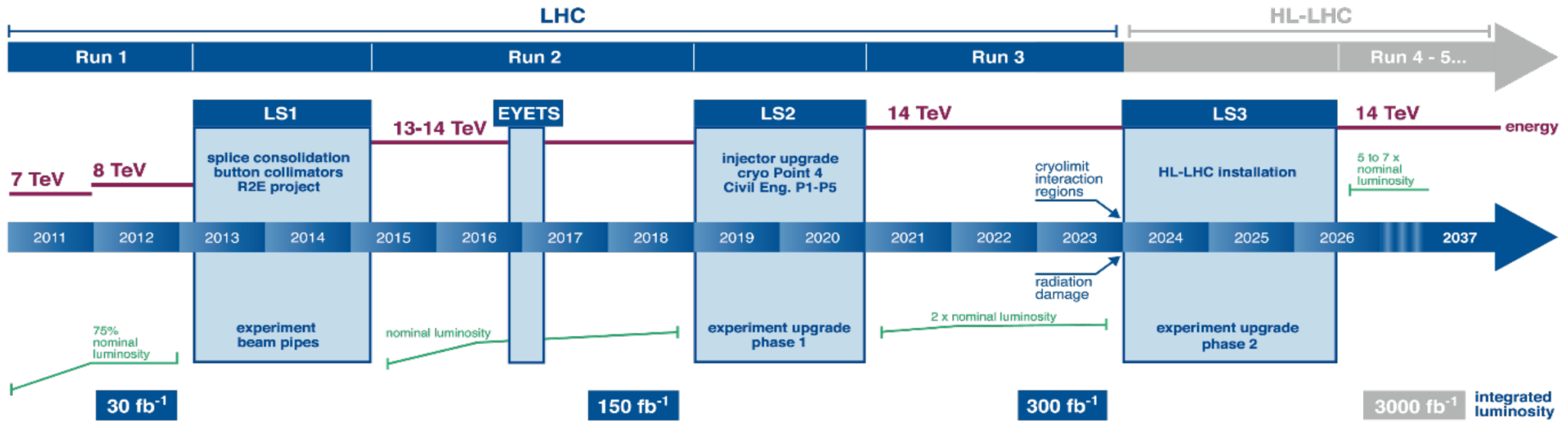
- Combination of 7 & 8 TeV results (BLUE comb.)

Par	Run1 combined		
	Value	Stat	Syst
$\phi_s$ [rad]	-0.090	0.078	0.041
$\Delta\Gamma_s$ [ps <sup>-1</sup> ]	0.085	0.011	0.007
$\Gamma_s$ [ps <sup>-1</sup> ]	0.675	0.003	0.003
$ A_{  }(0) ^2$	0.227	0.004	0.006
$ A_0(0) ^2$	0.522	0.003	0.007
$ A_S ^2$	0.072	0.007	0.018
$\delta_{\perp}$ [rad]	4.15	0.32	0.16
$\delta_{  }$ [rad]	3.15	0.10	0.05
$\delta_{\perp} - \delta_S$ [rad]	-0.08	0.03	0.01

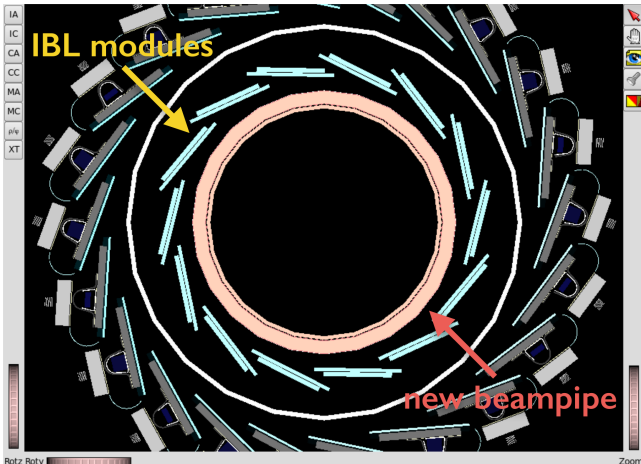


# Measurements in Run-2 and Beyond

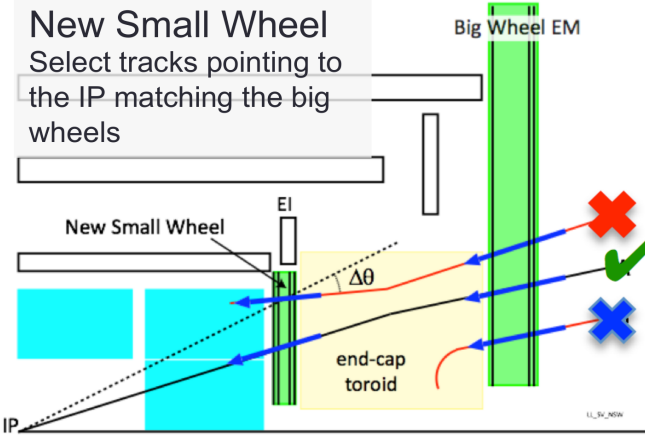
## LHC / HL-LHC Plan



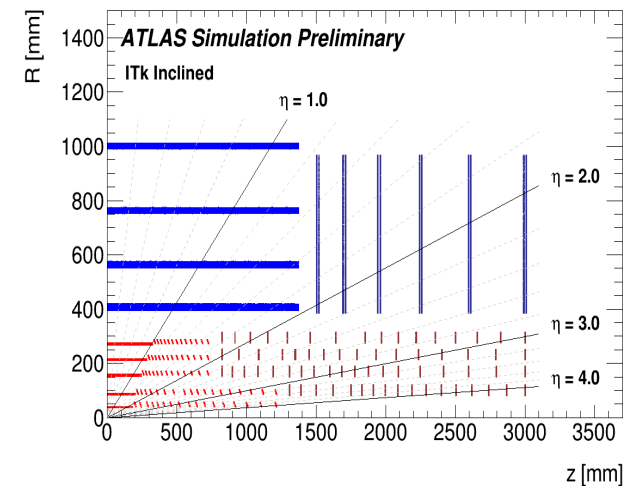
- New pixel layer (IBL, 32-38 mm) + small radius Be beam pipe
- Topological L1 trigger



- New small muon wheel
- Fast tracking trigger (FTK) at LVL 1.5; available in Run-2



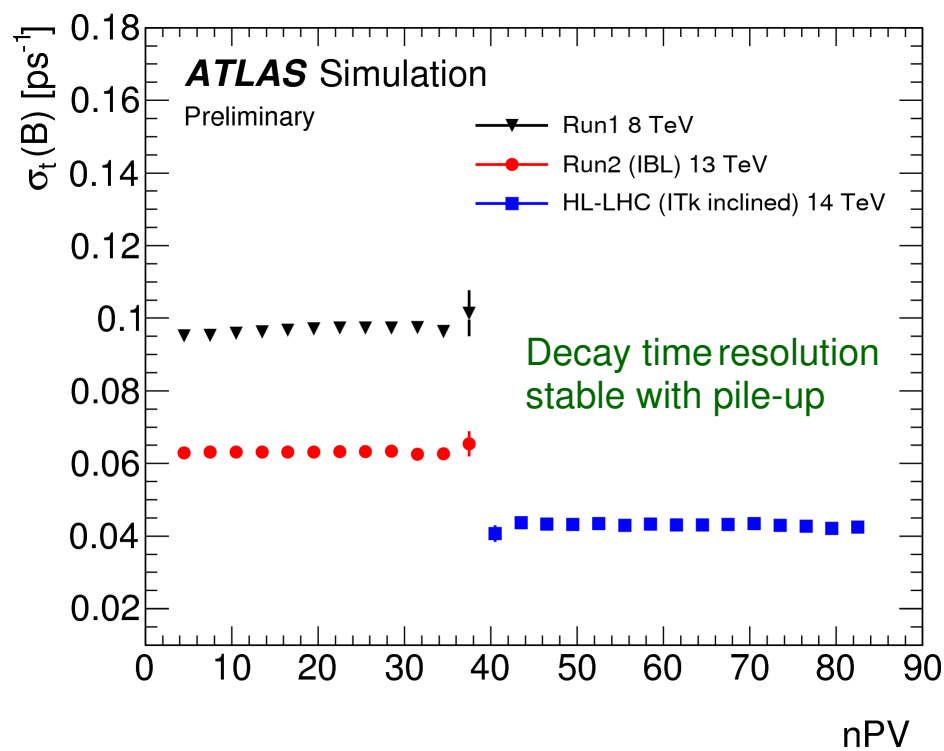
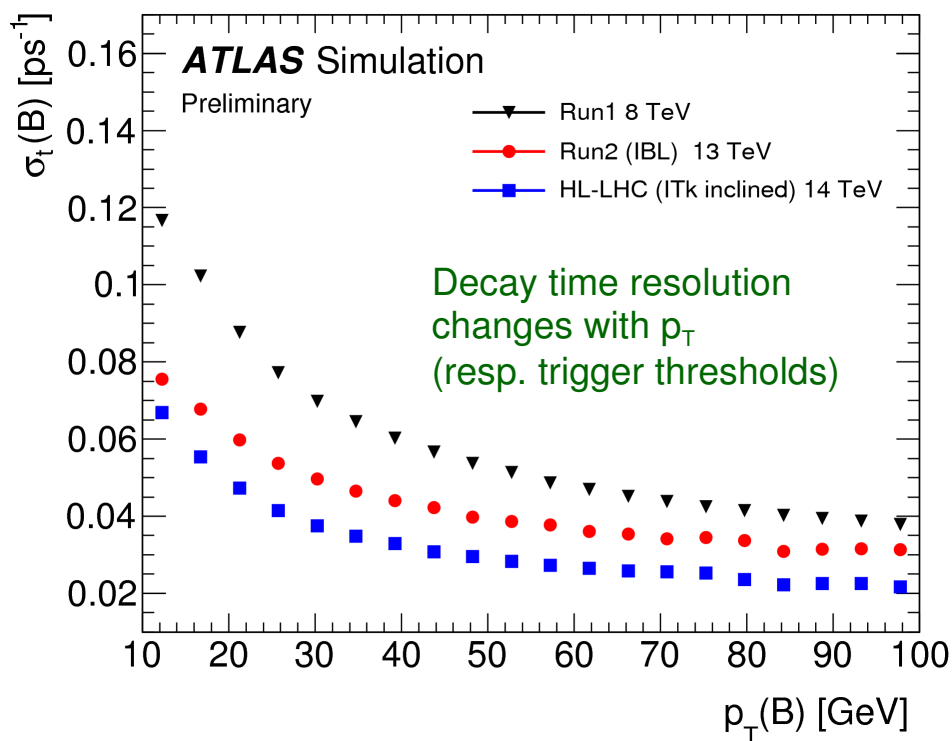
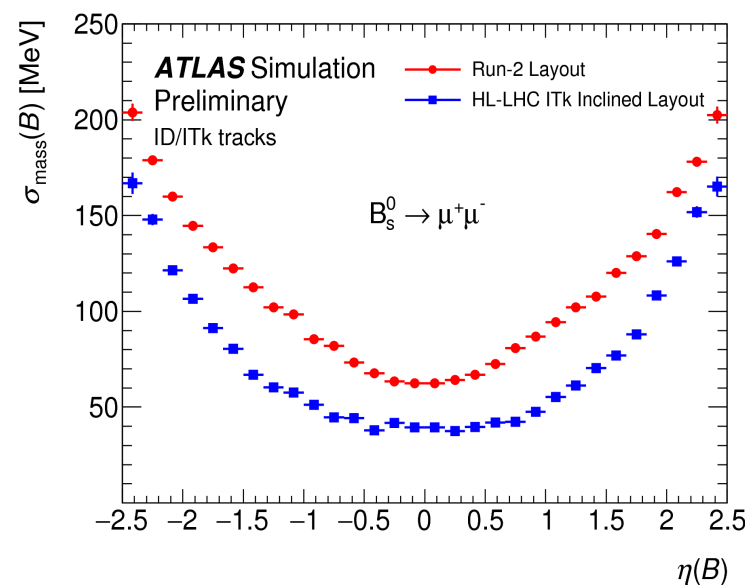
- Completely new Si based tracker (ITK)





# Detector Performance in Run-2 and Beyond

- **Resolution:** invariant mass in decay  $B_s \rightarrow \mu^+ \mu^-$ , proper decay time in  $B_s \rightarrow J/\psi(\mu^+ \mu^-) \phi(K^+ K^-)$  decay
- Comparison of Run-1, Run-2 (IBL) and HL-LHC (ITk) performances
- **Trigger:** use L1-topo (keep low thresholds at L1) and complicated HLT with full  $B_s \rightarrow J/\psi(\mu^+ \mu^-) \phi(K^+ K^-)$  decay topology reconstruction at trigger level





# Summary

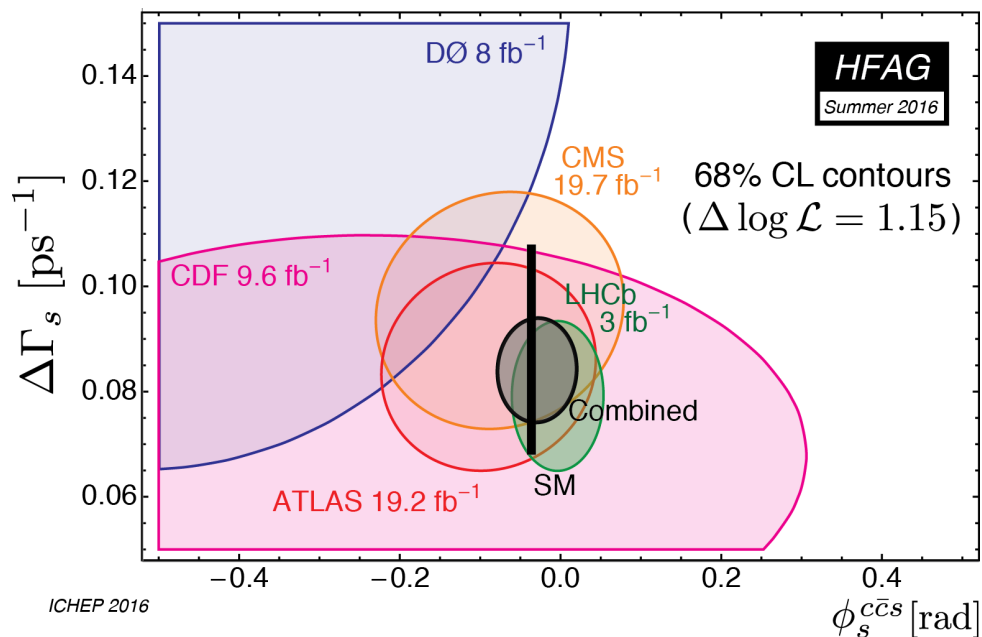
- ATLAS has measured  $\phi_s$  with full Run-1 dataset, combining 7 & 8 TeV pp collision data, in the decay channel  $B_s \rightarrow J/\psi(\mu^+\mu^-) \phi(K^+K^-)$ 
  - Results are consistent with Standard Model prediction as well as with other measurements:

$$\phi_s = -0.090 \pm 0.078 \text{ (stat.)} \pm 0.041 \text{ (syst.) rad}$$

$$\Delta\Gamma_s = 0.085 \pm 0.011 \text{ (stat.)} \pm 0.007 \text{ (syst.) ps}^{-1}$$

$$\Gamma_s = 0.675 \pm 0.003 \text{ (stat.)} \pm 0.003 \text{ (syst.) ps}^{-1}$$

JHEP 1608 (2016) 147



- The analysis is continuing in Run-2 and will continue also in the future stages of the LHC
  - Detector upgrades (namely in **tracking** and **muon system**) and new **trigger strategies** and tools will help to cope with the high-luminosity environment and achieve precision needed to examine possible beyond-SM effects



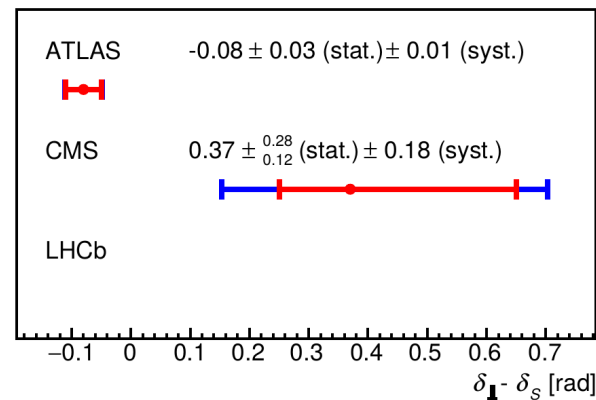
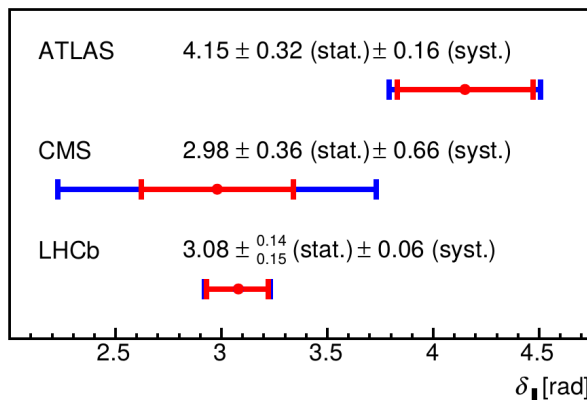
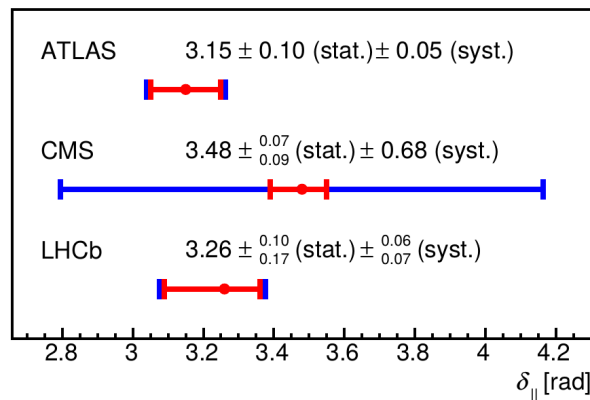
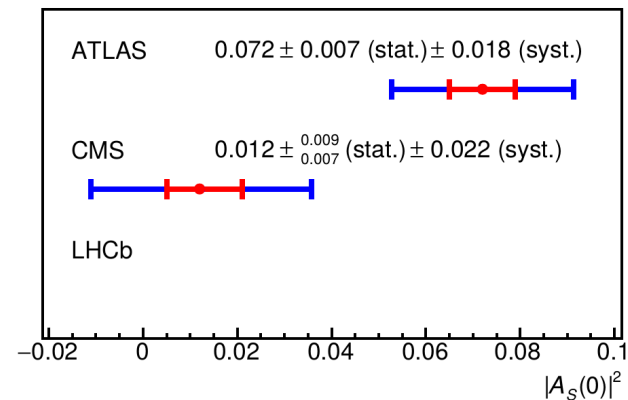
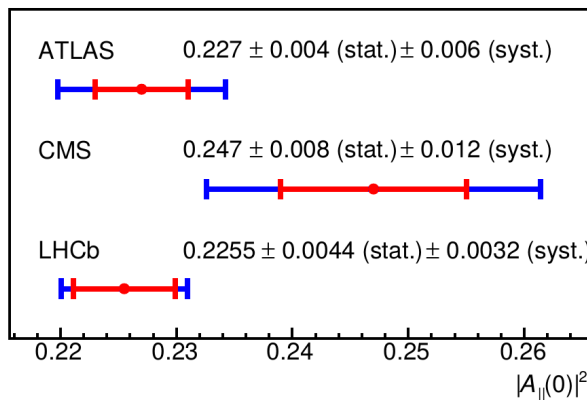
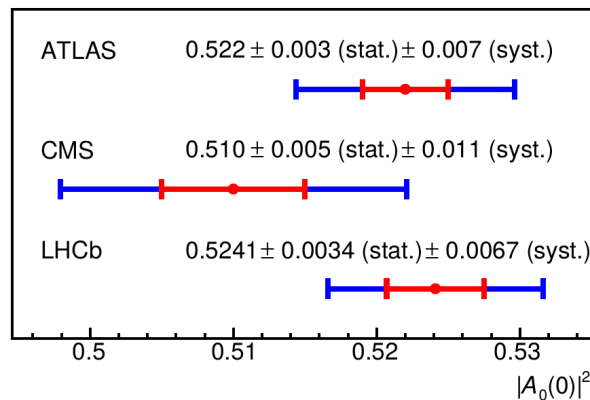
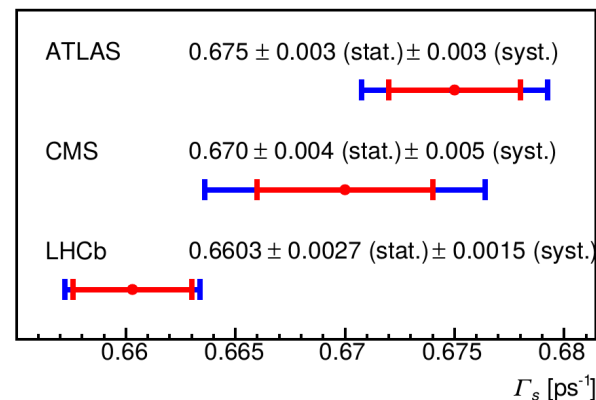
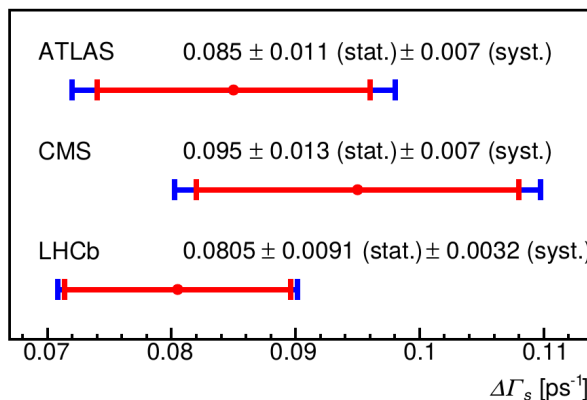
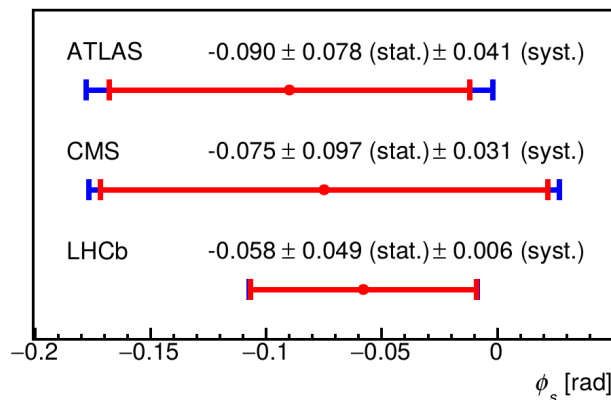


# Backup



# Comparison with Other Experiments

- $B_s \rightarrow J/\psi\phi(KK)$  channel: ATLAS JHEP 1608 (2016) 147, CMS PLB 757 (2016) 97, LHCb PRL 114 (2015) 041801





# Signal PDF

- Signal time-angular PDF:  
(convolved with detector resolution)

$$\frac{d^4\Gamma}{dt d\Omega} = \sum_{k=1}^{10} \mathcal{O}^{(k)}(t) g^{(k)}(\theta_T, \psi_T, \phi_T)$$

2 PDFs for  $B_s$  and  $\bar{B}_s$  (alternative  $\pm$  signs): PDF( $B_s$ ), PDF( $\bar{B}_s$ )  
 Tagged fit: Prob( $B_s$ -tag)\*PDF( $B_s$ ) + (1-Prob( $B_s$ -tag))\*PDF( $\bar{B}_s$ )  
 Untagged fit: Prob( $B_s$ -tag) = 0.5

Symmetries:  $\{\phi_s, \Delta\Gamma_s, \delta_\perp, \delta_\parallel\} \rightarrow \{\pi - \phi_s, -\Delta\Gamma_s, \pi - \delta_\perp, 2\pi - \delta_\parallel\}$   
 ~~$\{\phi_s, \Delta\Gamma_s, \delta_\perp, \delta_\parallel, \delta_S\} \rightarrow \{\phi_s, \Delta\Gamma_s, \pi - \delta_\perp, -\delta_\parallel, -\delta_S\}$  (untagged fit only)~~

	$k$	$\mathcal{O}^{(k)}(t)$	$g^{(k)}(\theta_T, \psi_T, \phi_T)$
CP +1 CP +1 CP -1	1	$\frac{1}{2} A_0(0) ^2 \left[ (1 + \cos \phi_s) e^{-\Gamma_L^{(s)} t} + (1 - \cos \phi_s) e^{-\Gamma_H^{(s)} t} \pm 2e^{-\Gamma_s t} \sin(\Delta m_s t) \sin \phi_s \right]$	$2 \cos^2 \psi_T (1 - \sin^2 \theta_T \cos^2 \phi_T)$
	2	$\frac{1}{2} A_\parallel(0) ^2 \left[ (1 + \cos \phi_s) e^{-\Gamma_L^{(s)} t} + (1 - \cos \phi_s) e^{-\Gamma_H^{(s)} t} \pm 2e^{-\Gamma_s t} \sin(\Delta m_s t) \sin \phi_s \right]$	$\sin^2 \psi_T (1 - \sin^2 \theta_T \sin^2 \phi_T)$
	3	$\frac{1}{2} A_\perp(0) ^2 \left[ (1 - \cos \phi_s) e^{-\Gamma_L^{(s)} t} + (1 + \cos \phi_s) e^{-\Gamma_H^{(s)} t} \mp 2e^{-\Gamma_s t} \sin(\Delta m_s t) \sin \phi_s \right]$	$\sin^2 \psi_T \sin^2 \theta_T$
Interference terms	4	$\frac{1}{2} A_0(0)  A_\parallel(0)  \cos \delta_\parallel \left[ (1 + \cos \phi_s) e^{-\Gamma_L^{(s)} t} + (1 - \cos \phi_s) e^{-\Gamma_H^{(s)} t} \pm 2e^{-\Gamma_s t} \sin(\Delta m_s t) \sin \phi_s \right]$	$\frac{1}{\sqrt{2}} \sin 2\psi_T \sin^2 \theta_T \sin 2\phi_T$
	5	$ A_\parallel(0)  A_\perp(0)  \left[ \frac{1}{2}(e^{-\Gamma_L^{(s)} t} - e^{-\Gamma_H^{(s)} t}) \cos(\delta_\perp - \delta_\parallel) \sin \phi_s \pm e^{-\Gamma_s t} (\sin(\delta_\perp - \delta_\parallel) \cos(\Delta m_s t) - \cos(\delta_\perp - \delta_\parallel) \cos \phi_s \sin(\Delta m_s t)) \right]$	$-\sin^2 \psi_T \sin 2\theta_T \sin \phi_T$
	6	$ A_0(0)  A_\perp(0)  \left[ \frac{1}{2}(e^{-\Gamma_L^{(s)} t} - e^{-\Gamma_H^{(s)} t}) \cos \delta_\perp \sin \phi_s \pm e^{-\Gamma_s t} (\sin \delta_\perp \cos(\Delta m_s t) - \cos \delta_\perp \cos \phi_s \sin(\Delta m_s t)) \right]$	$\frac{1}{\sqrt{2}} \sin 2\psi_T \sin 2\theta_T \cos \phi_T$
S-wave terms	7	$\frac{1}{2} A_S(0) ^2 \left[ (1 - \cos \phi_s) e^{-\Gamma_L^{(s)} t} + (1 + \cos \phi_s) e^{-\Gamma_H^{(s)} t} \mp 2e^{-\Gamma_s t} \sin(\Delta m_s t) \sin \phi_s \right]$	$\frac{2}{3} (1 - \sin^2 \theta_T \cos^2 \phi_T)$
	8	$ A_S(0)  A_\parallel(0)  \left[ \frac{1}{2}(e^{-\Gamma_L^{(s)} t} - e^{-\Gamma_H^{(s)} t}) \sin(\delta_\parallel - \delta_S) \sin \phi_s \pm e^{-\Gamma_s t} (\cos(\delta_\parallel - \delta_S) \cos(\Delta m_s t) - \sin(\delta_\parallel - \delta_S) \cos \phi_s \sin(\Delta m_s t)) \right]$	$\frac{1}{3} \sqrt{6} \sin \psi_T \sin^2 \theta_T \sin 2\phi_T$
	9	$\frac{1}{2} A_S(0)  A_\perp(0)  \sin(\delta_\perp - \delta_S) \left[ (1 - \cos \phi_s) e^{-\Gamma_L^{(s)} t} + (1 + \cos \phi_s) e^{-\Gamma_H^{(s)} t} \mp 2e^{-\Gamma_s t} \sin(\Delta m_s t) \sin \phi_s \right]$	$\frac{1}{3} \sqrt{6} \sin \psi_T \sin 2\theta_T \cos \phi_T$
	10	$ A_0(0)  A_S(0)  \left[ \frac{1}{2}(e^{-\Gamma_H^{(s)} t} - e^{-\Gamma_L^{(s)} t}) \sin \delta_S \sin \phi_s \pm e^{-\Gamma_s t} (\cos \delta_S \cos(\Delta m_s t) + \sin \delta_S \cos \phi_s \sin(\Delta m_s t)) \right]$	$\frac{4}{3} \sqrt{3} \cos \psi_T (1 - \sin^2 \theta_T \cos^2 \phi_T)$



# Unbinned Maximum Likelihood Fit

$$\ln \mathcal{L} = \sum_{i=1}^N \left\{ w_i \cdot \ln(f_s \cdot \mathcal{F}_s(m_i, t_i, \sigma_{t_i}, \Omega_i, P(B|Q), p_{T_i})) \right. \\ \left. + f_s \cdot f_{B^0} \cdot \mathcal{F}_{B^0}(m_i, t_i, \sigma_{t_i}, \Omega_i, P(B|Q), p_{T_i}) \right. \\ \left. + f_s \cdot f_{\Lambda_b} \cdot \mathcal{F}_{\Lambda_b}(m_i, t_i, \sigma_{t_i}, \Omega_i, P(B|Q), p_{T_i}) \right. \\ \left. + (1 - f_s \cdot (1 + f_{B^0} + f_{\Lambda_b})) \cdot \mathcal{F}_{\text{bkg}}(m_i, t_i, \sigma_{t_i}, \Omega_i, P(B|Q), p_{T_i}) \right\}$$

## Signal decay main parameters:

- CP violating phase  $\phi_s$
- Decay width  $\Gamma_s = (\Gamma_H + \Gamma_L)/2$
- Decay width difference  $\Delta\Gamma = \Gamma_H - \Gamma_L$
- CP state amplitudes  $|A_0(0)|^2$  and  $|A_{||}(0)|^2$
- Strong phases  $\delta_{||}$  and  $\delta_{\perp}$
- S-wave amplitude  $|A_S(0)|^2$  and phase  $\delta_S$  (fitting  $\delta_S - \delta_{\perp}$  to avoid high correlations)
- $B_s$  mean mass
- ( $\Delta m_s$  fixed to  $17.77 \text{ ps}^{-1}$ )

Weights accounting for **proper decay time trigger efficiency** (muons track  $d_0$  reconstruction efficiency bias); estimated from MC

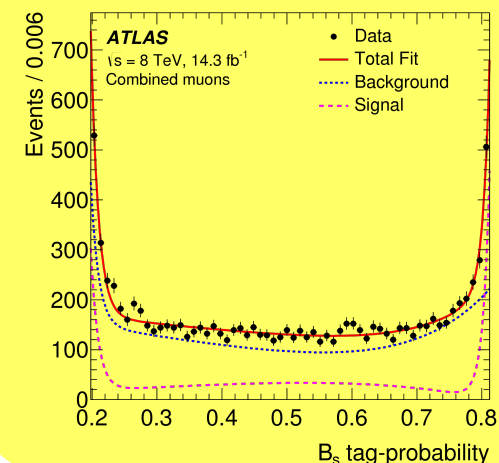
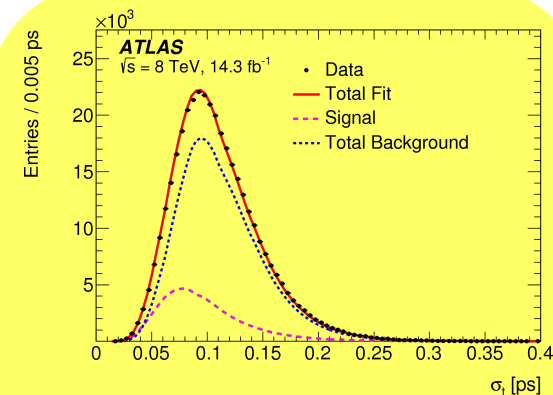
**Combinatorial background** description, derived from data sidebands; angular distribution described by spherical harmonics and fixed in the fit

**$B_d \rightarrow J/\psi K^*(K\pi)$  and  $\Lambda_b \rightarrow J/\psi \Lambda^*(Kp)$  decay reflections**, derived from MC, PDG and the LHCb  $\Lambda_b \rightarrow J/\psi Kp$  measurement; fixed shape and relative contribution in the fit

Signal and background PDFs for conditional observables determined from data using sidebands subtraction; PDFs fixed in the fit

## Measured variables:

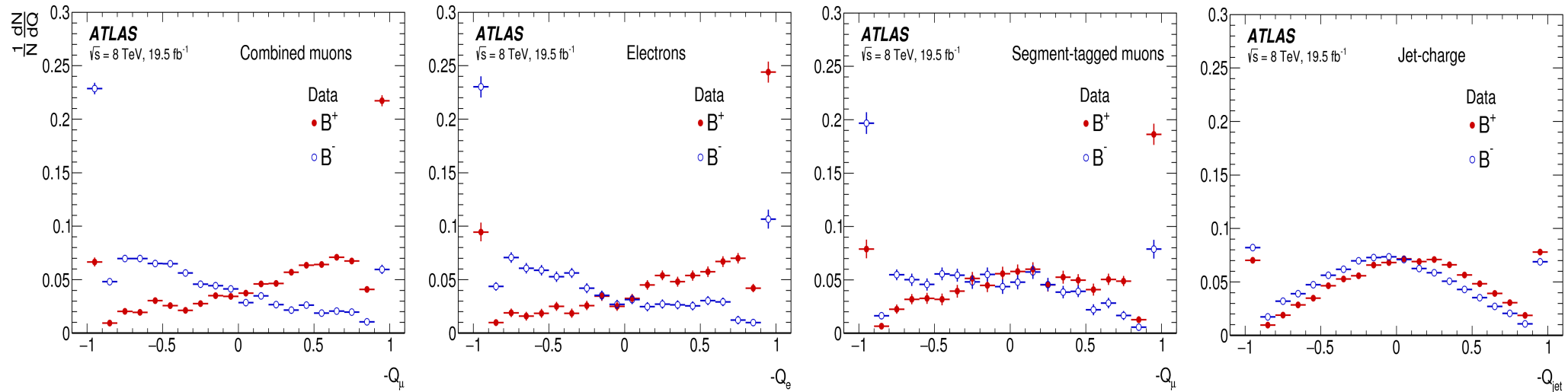
- $B_s$  mass  $m_i$
- $B_s$  proper decay time  $t_i$  and its uncertainty  $\sigma_{t_i}$
- 3 angles  $\Omega_i (\theta_{T_i}, \phi_{T_i}, \psi_{T_i})$
- $B_s$  momentum  $p_{T_i}$
- $B_s$  tag probability  $p_{B|Q_i}$
- tagging method  $M_i$



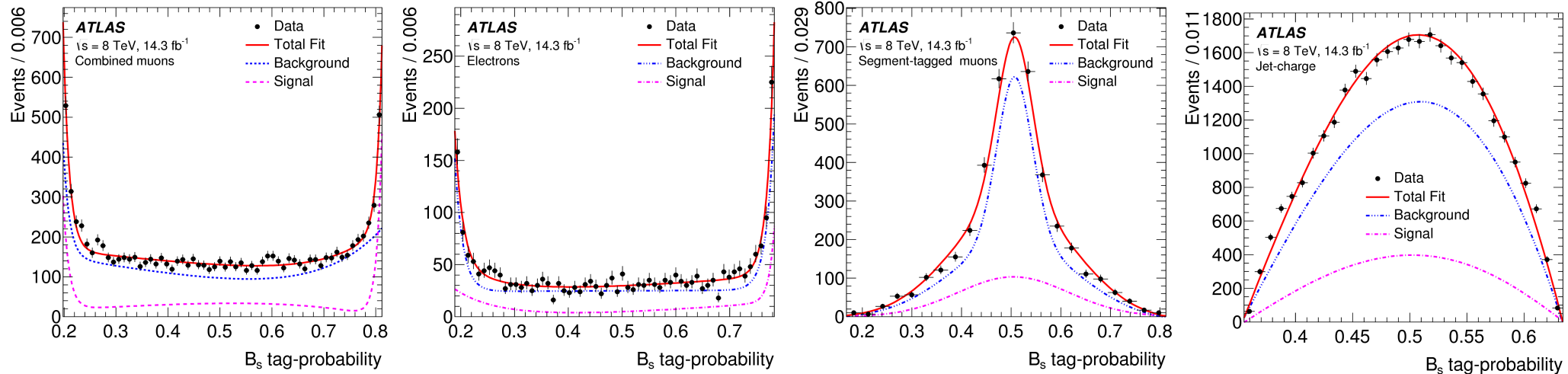


# B-Flavour Tagging Distributions

- Cone charge for the calibration  $B^+$  and  $B^-$  data samples



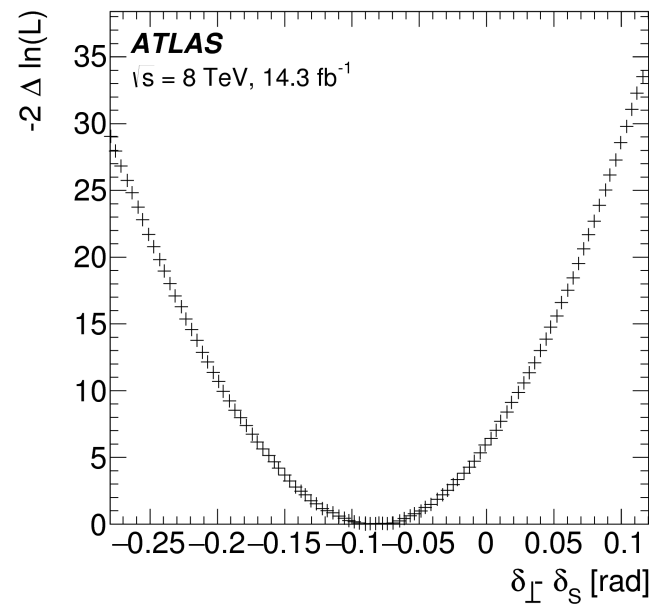
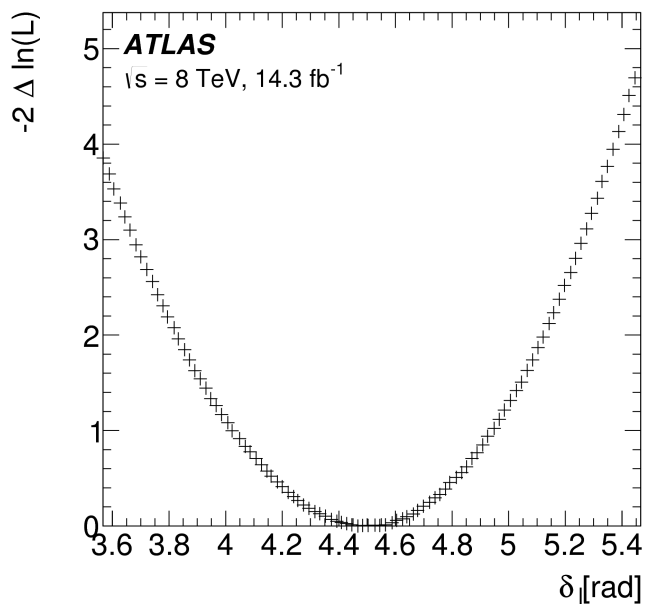
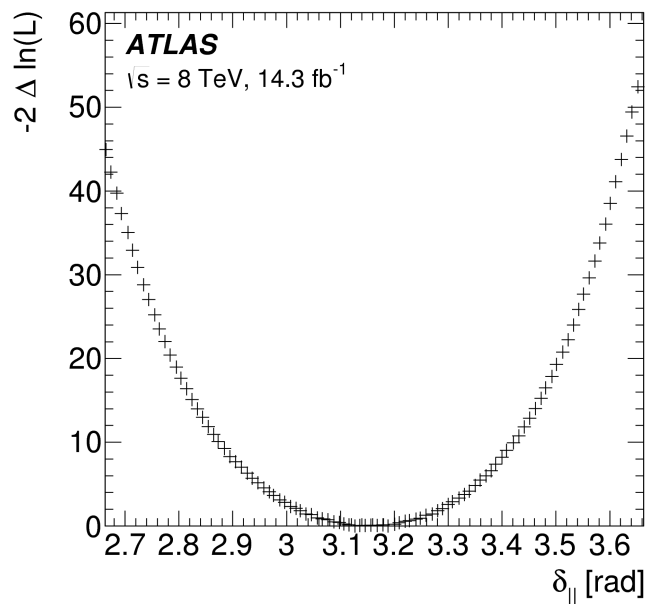
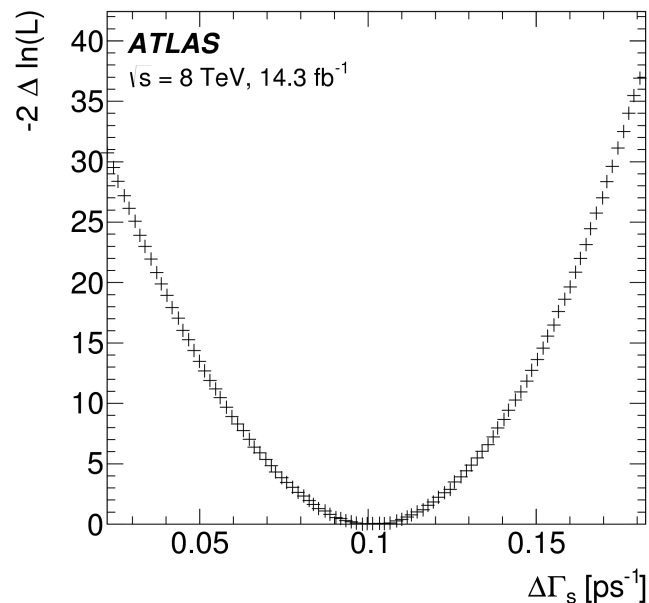
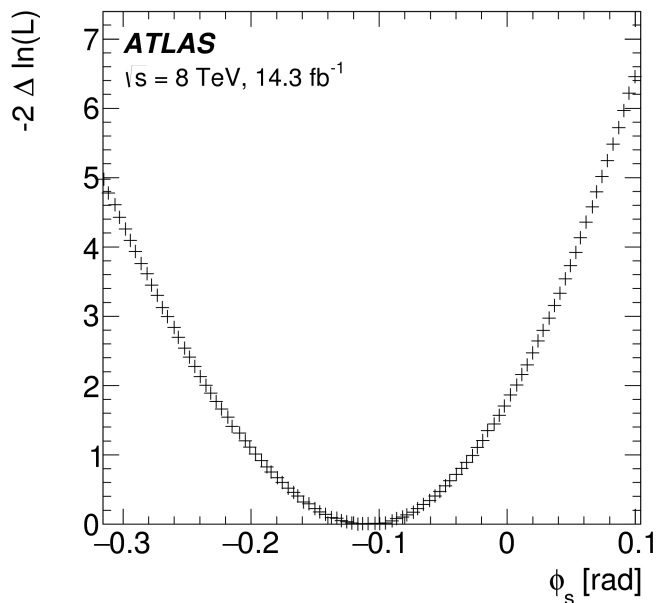
- $B_s$ -tag probability distribution in the fit, signal & background obtained using sidebands-subtraction method on the real data





# 1D Likelihood Scans

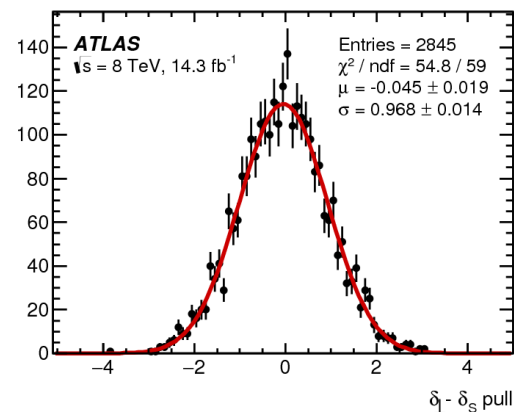
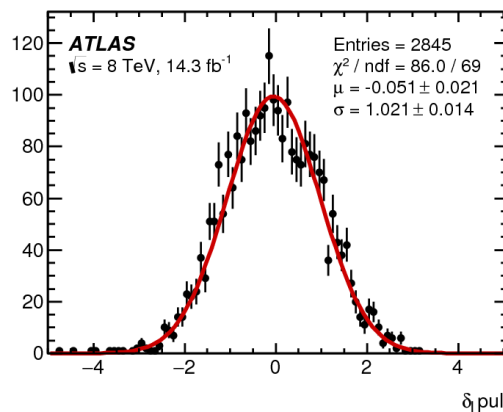
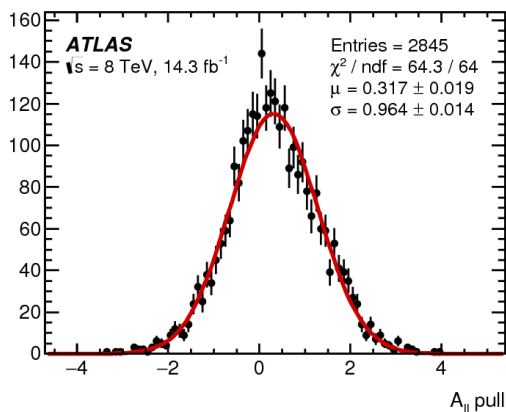
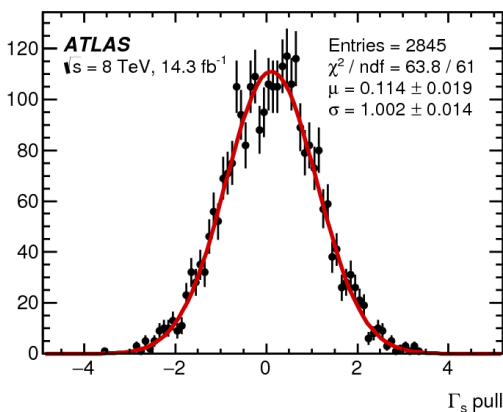
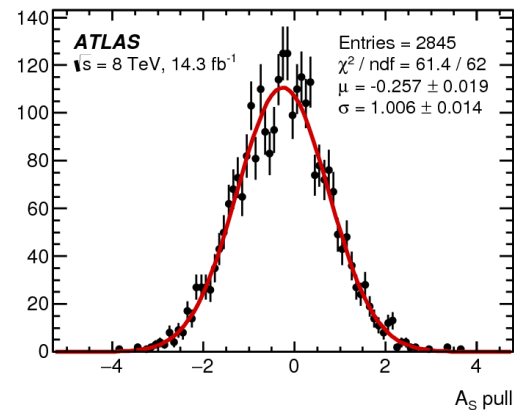
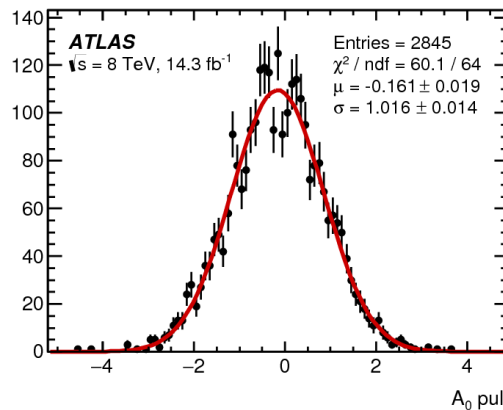
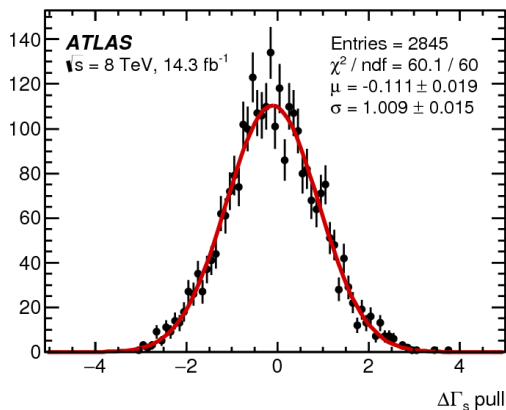
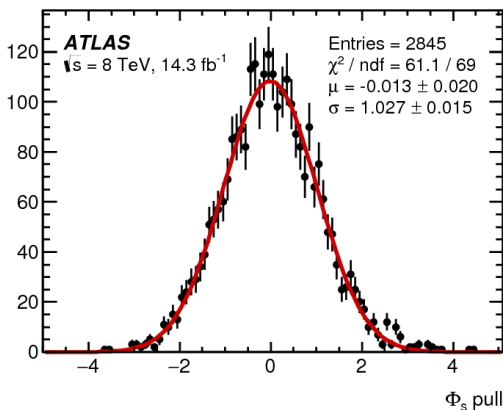
- Cross-check of the Gaussian behavior of the likelihood, resp. asymmetry of the errors





# UML Fit Pulls

- Cross-check of the self-consistency of the Unbinned Maximum Likelihood fit



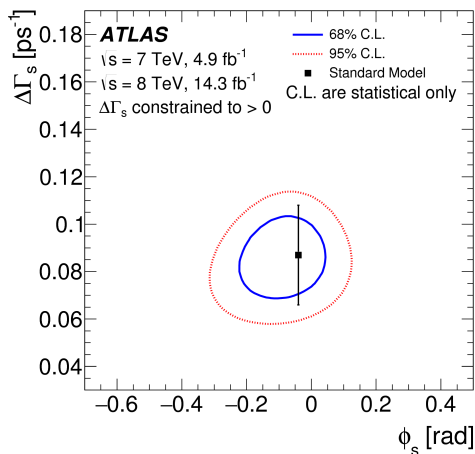


# ATLAS $\phi_s$ Measurements in Run-1

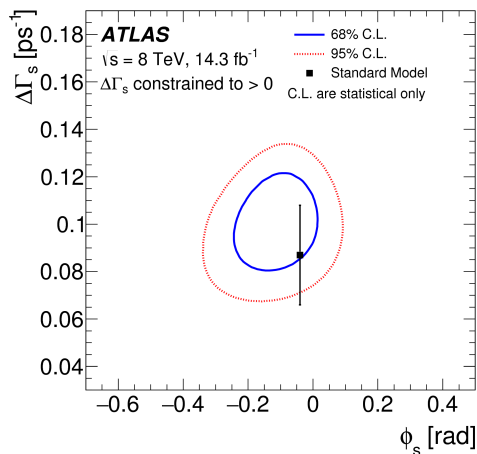
- Comparison of the 7 and 8 TeV tagged analyses with the combination

Par	8 TeV data			7 TeV data			Run1 combined		
	Value	Stat	Syst	Value	Stat	Syst	Value	Stat	Syst
$\phi_s$ [rad]	-0.110	0.082	0.042	0.12	0.25	0.05	-0.090	0.078	0.041
$\Delta\Gamma_s$ [ps <sup>-1</sup> ]	0.101	0.013	0.007	0.053	0.021	0.010	0.085	0.011	0.007
$\Gamma_s$ [ps <sup>-1</sup> ]	0.676	0.004	0.004	0.677	0.007	0.004	0.675	0.003	0.003
$ A_{\parallel}(0) ^2$	0.230	0.005	0.006	0.220	0.008	0.009	0.227	0.004	0.006
$ A_0(0) ^2$	0.520	0.004	0.007	0.529	0.006	0.012	0.522	0.003	0.007
$ A_S ^2$	0.097	0.008	0.022	0.024	0.014	0.028	0.072	0.007	0.018
$\delta_{\perp}$ [rad]	4.50	0.45	0.30	3.89	0.47	0.11	4.15	0.32	0.16
$\delta_{\parallel}$ [rad]	3.15	0.10	0.05	[3.04, 3.23]		0.09	3.15	0.10	0.05
$\delta_{\perp} - \delta_S$ [rad]	-0.08	0.03	0.01	[3.02, 3.25]		0.04	-0.08	0.03	0.01

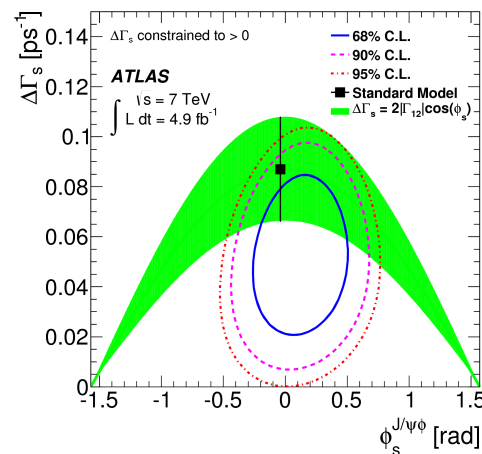
7 & 8 TeV  
JHEP 1608 (2016) 147



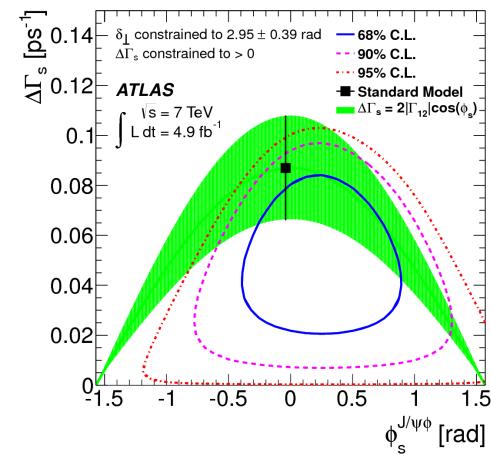
8 TeV  
JHEP 1608 (2016) 147



7 TeV  
PRD 90 (2014) 052007



7 TeV (untagged)  
JHEP 12 (2012) 072

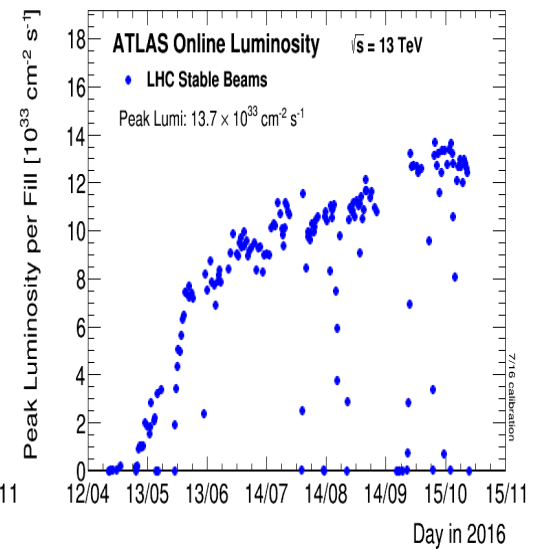
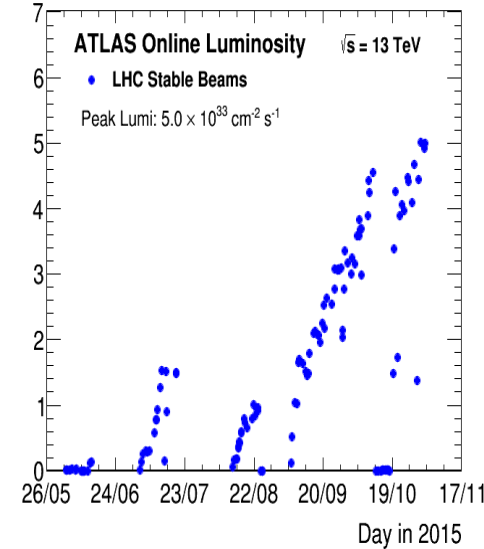
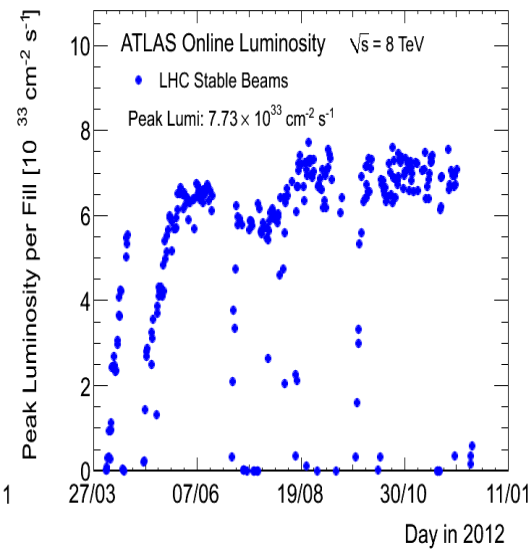
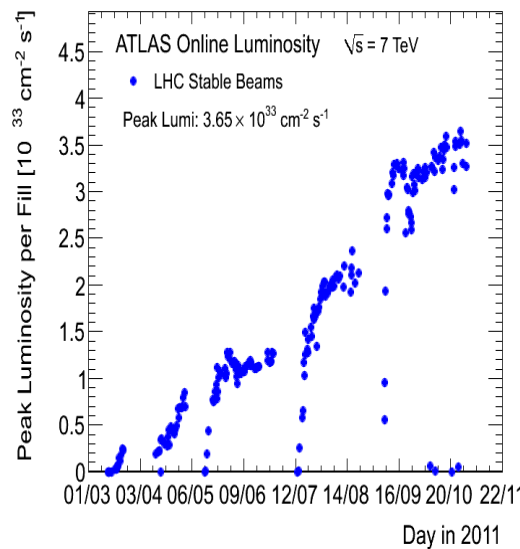
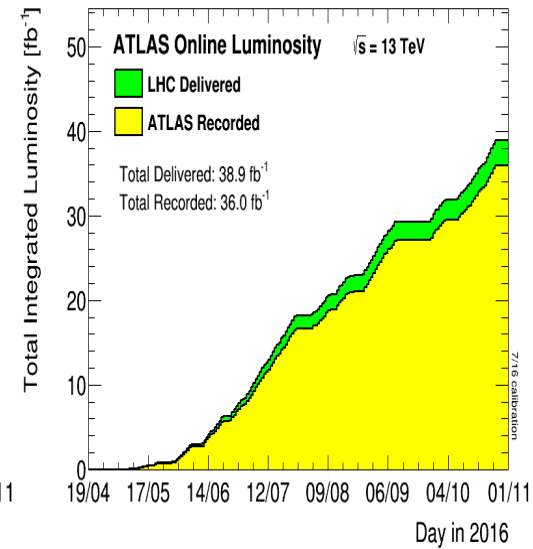
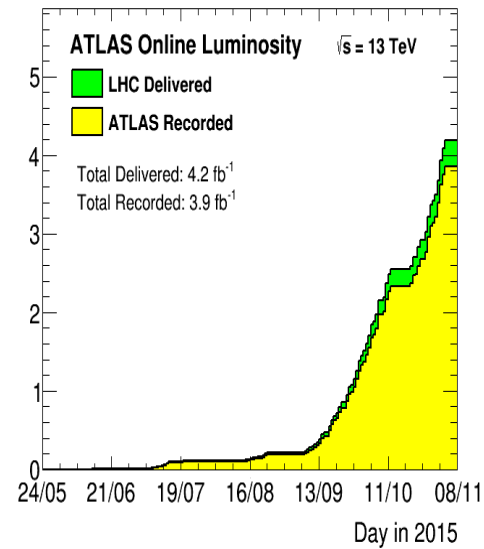
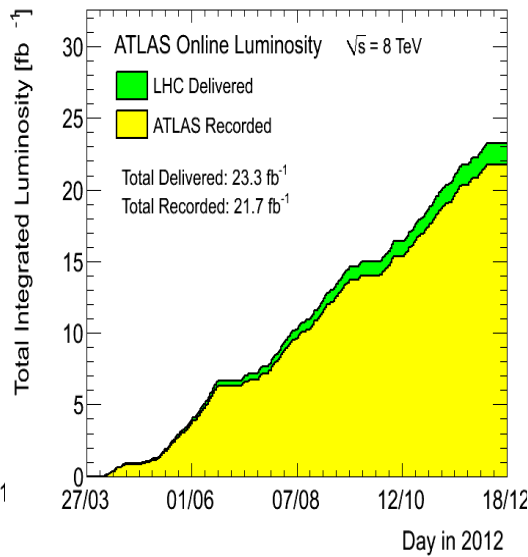
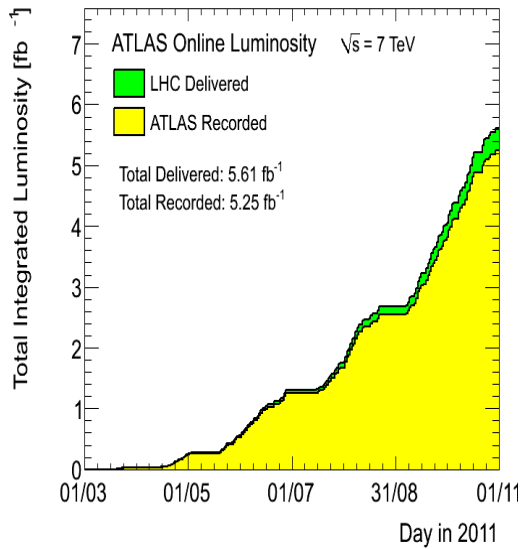






# Data Taking (pp): Run-1 and Run-2

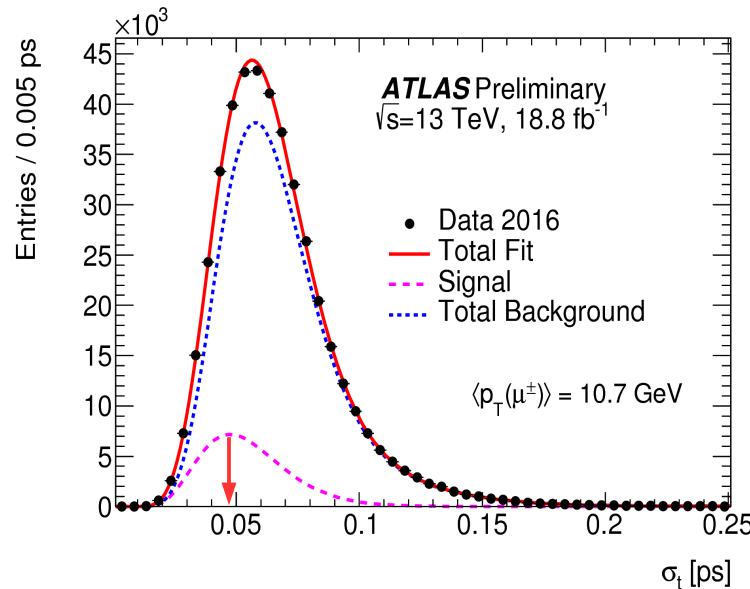
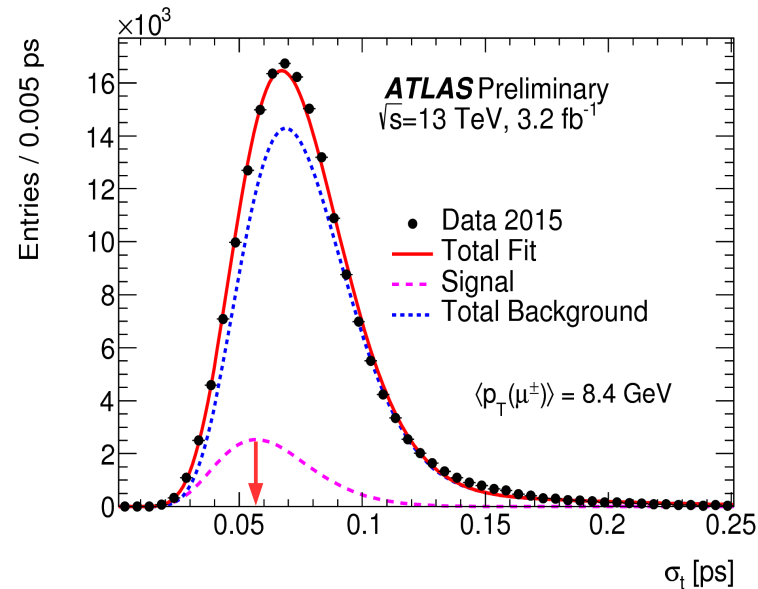
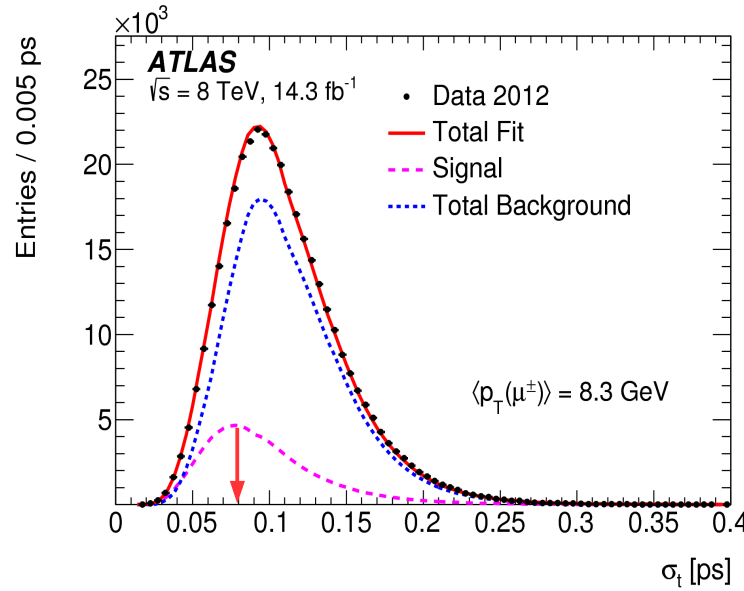
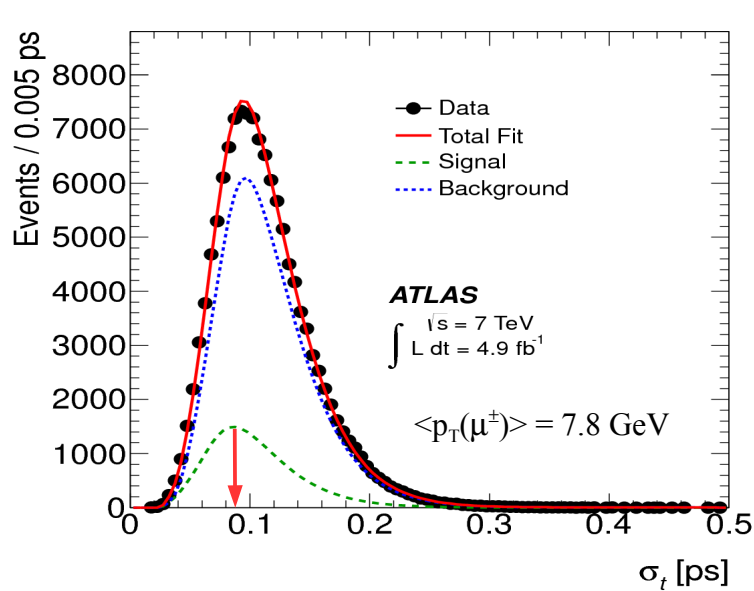
- 7 TeV data, 5.08 fb<sup>-1</sup>  
50ns, 3.7×10<sup>33</sup> cm<sup>-2</sup>s<sup>-1</sup>
- 8 TeV, 21.3 fb<sup>-1</sup>  
50ns, 7.7×10<sup>33</sup> cm<sup>-2</sup>s<sup>-1</sup>
- 13 TeV (2015), 3.9 fb<sup>-1</sup>  
50/25ns, 5.0×10<sup>33</sup> cm<sup>-2</sup>s<sup>-1</sup>
- 13 TeV (2016), 36.0 fb<sup>-1</sup>  
25ns, 13.7×10<sup>33</sup> cm<sup>-2</sup>s<sup>-1</sup>





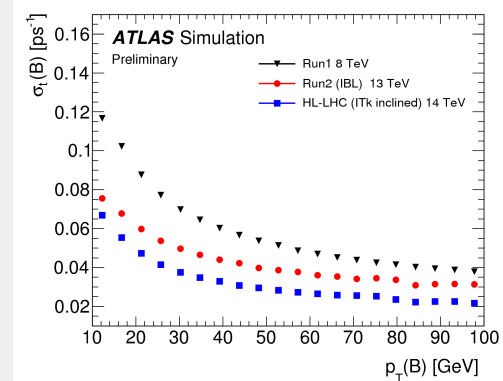
# Proper Decay Time Resolution in Real Data

- Comparison of the proper decay time resolution distributions in Run-1 and Run-2 data:



**Average proper decay time distribution driven by:**

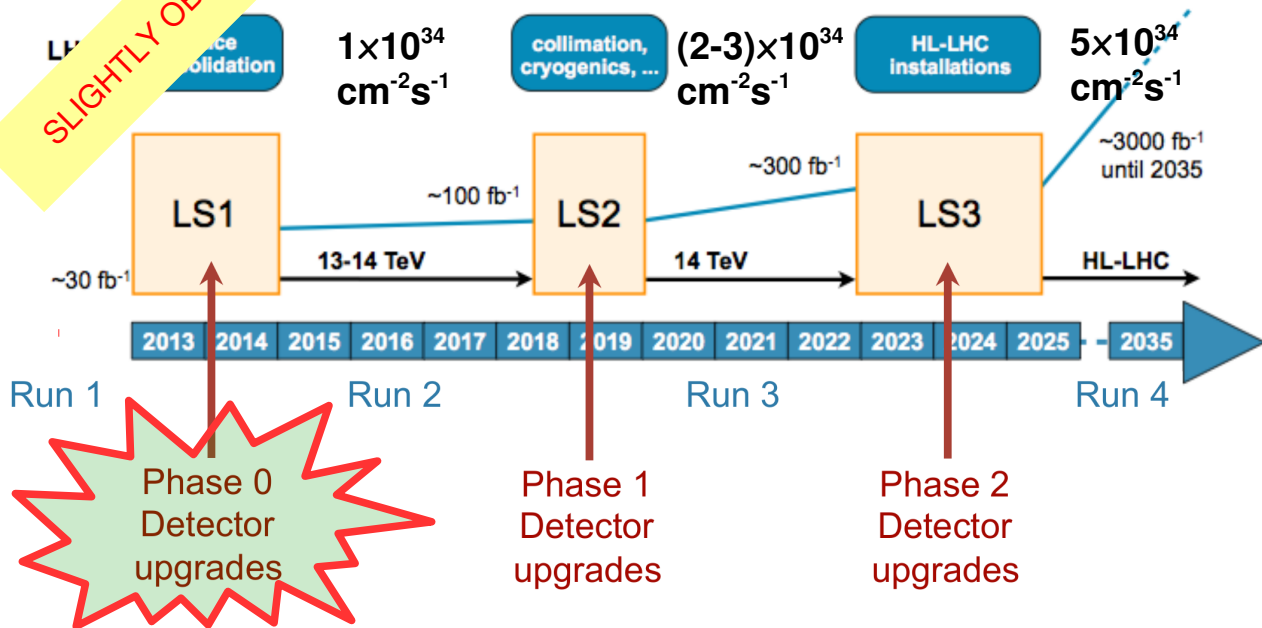
- Tracking performance (with or without IBL)
- Trigger muon  $p_T$  thresholds  $\rightarrow$  average  $B_s$ -meson momentum



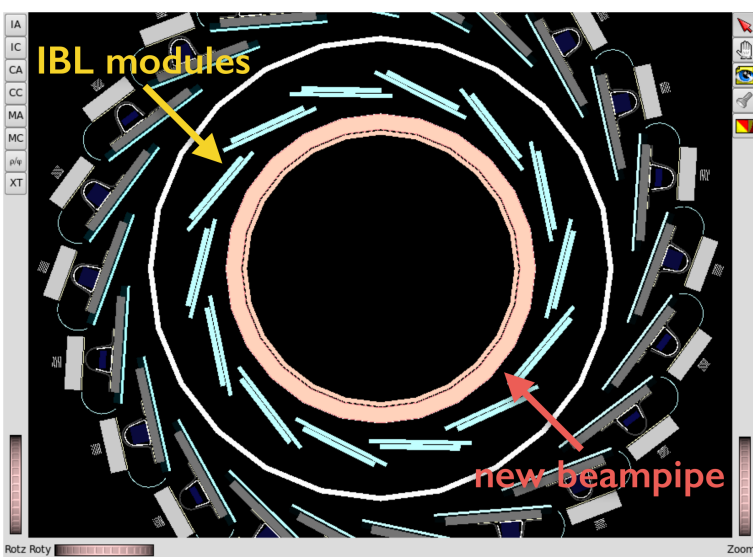


# Detector & Trigger Upgrades - Phase 0

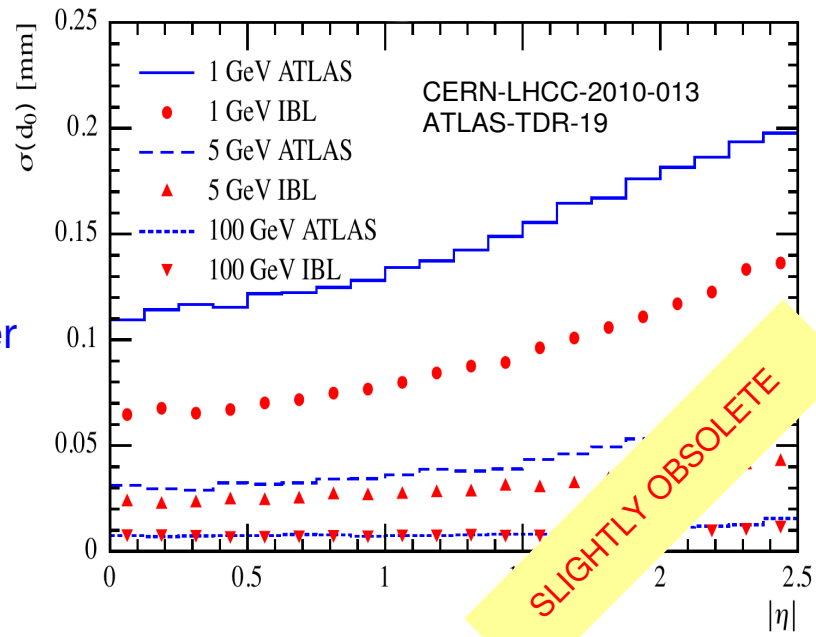
SLIGHTLY OBSOLETE



- Long Shutdown (LS) 1 almost over, LHC starts providing physics data in Spring 2015
- **Additional Pixel Layer (IBL)** and Be small radius beam pipe
- **Topological L1 trigger**
- Improved coverage of Muon spectrometer ( $1.0 < |\eta| < 1.3$ )
- Diamond Beam Monitor, consolidation of some parts of the detector (cooling etc.)



- Small radius (32-38 mm; current B-layer at 50.5 mm), small material budget
- 4<sup>th</sup> pixel layer => more robust track reconstruction, better impact parameter  $d_0$  and  $z_0$  resolution
- Better  $\theta$  and  $\phi$  resolution at low  $p_T \sim 1$  GeV

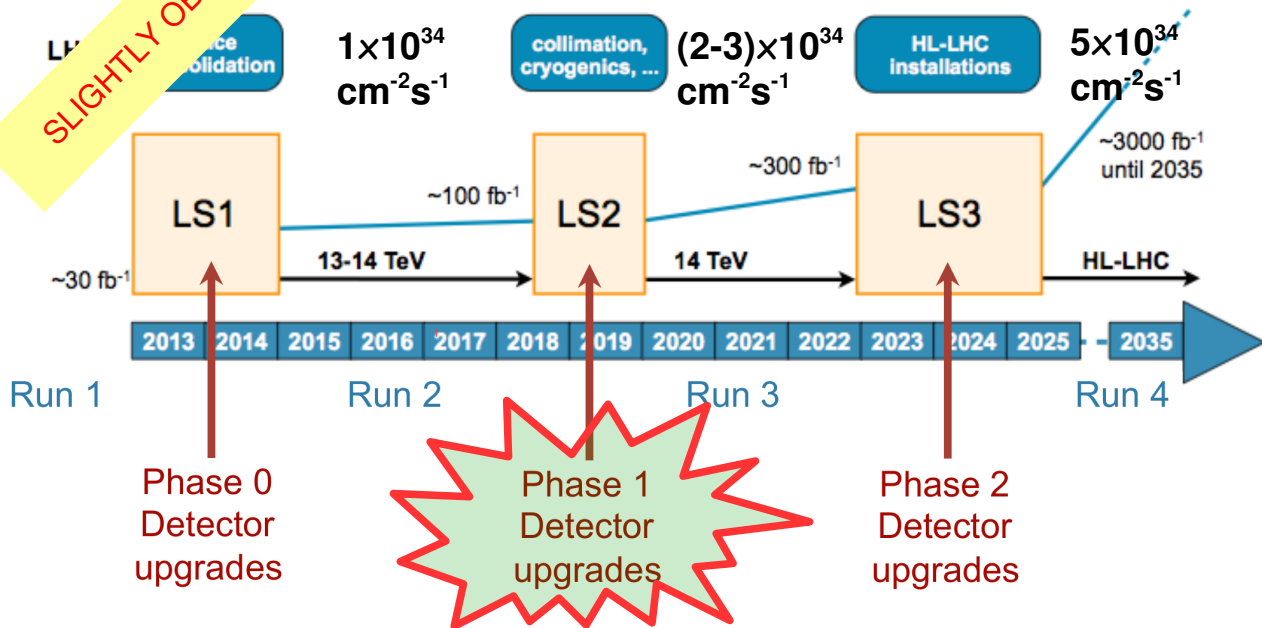


SLIGHTLY OBSOLETE



# Detector & Trigger Upgrades - Phase 1

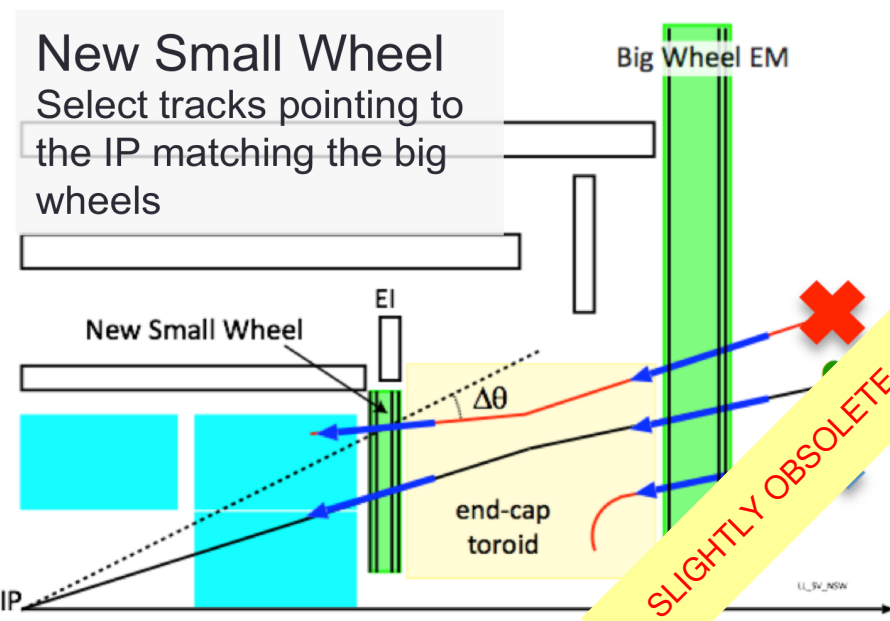
SLIGHTLY OBSOLETE



- Goal: no loss of performance when going above LHC nominal luminosity
- **New small muon wheel**
- **New fast-tracking (FTK) at trigger level 1.5. Gradually implemented already during Run 2**
- Higher granularity and precision L1 trigger for calorimeter
- TDAQ improved performance

## Fast tracking trigger:

- HW based track finder in the Inner Detector silicon layers at “offline precision”
- Provides tracks already before the L2 trigger (first SW based trigger layer)
- Two-step processing: hit pattern matching & subsequent linear fitting in FPGAs

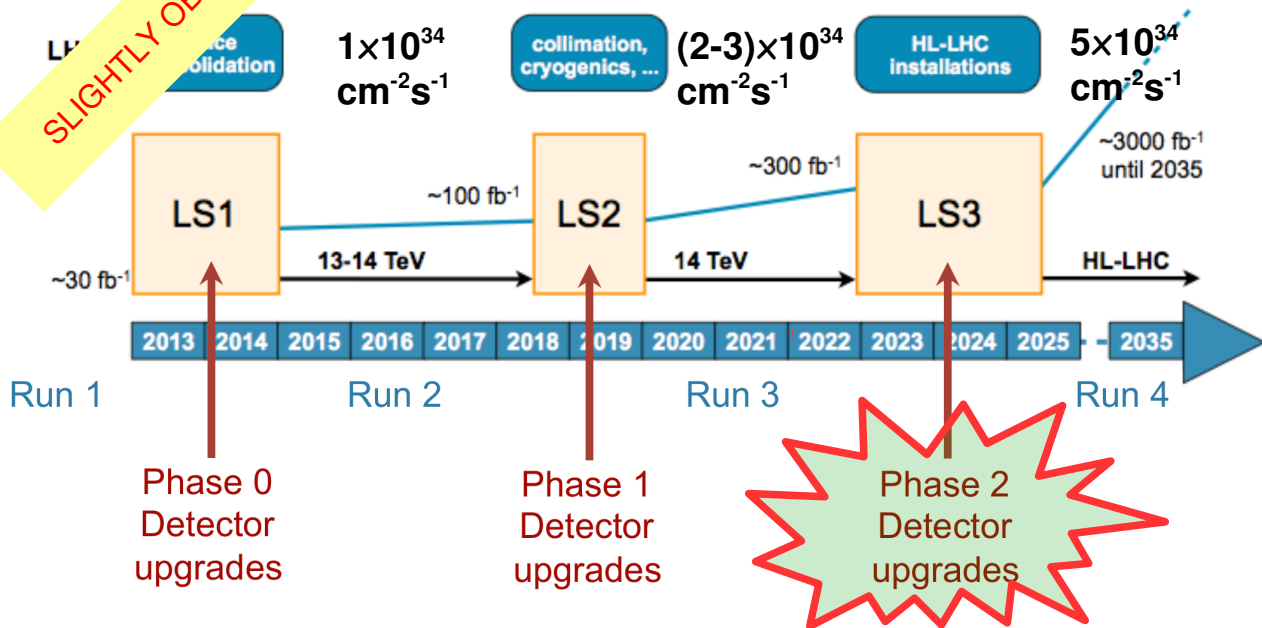


SLIGHTLY OBSOLETE



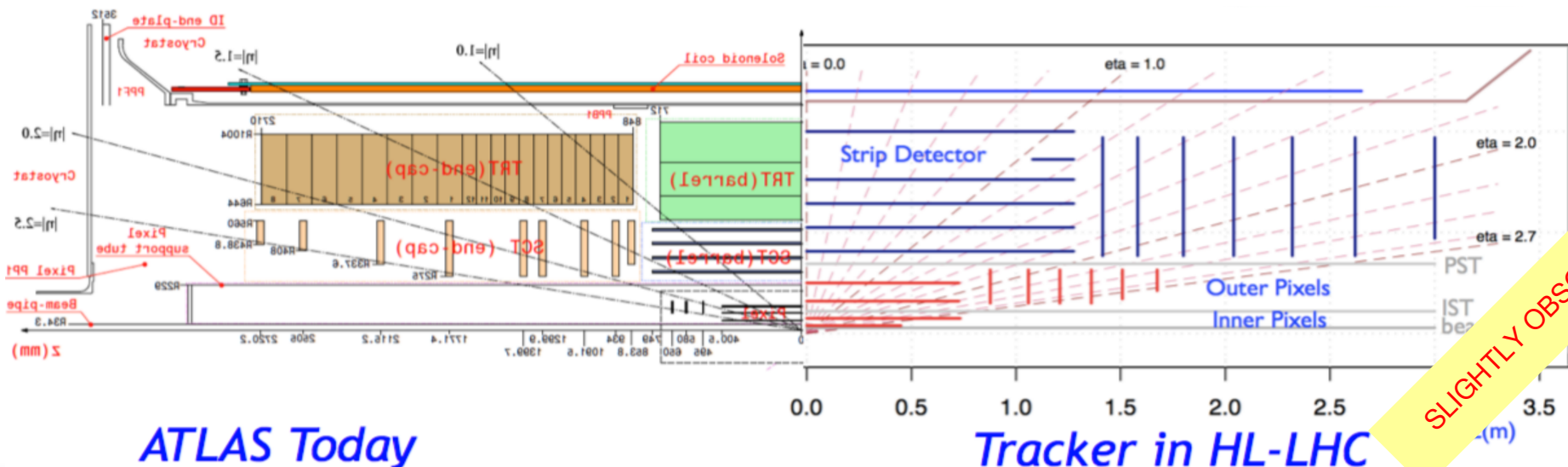
# Detector & Trigger Upgrades - Phase 2

SLIGHTLY OBSOLETE



- Goal: maintain/improve performance despite high lumi.
- **Completely new Si based tracking (ITK)**
- New trigger system – possibly will include HW-based L1 track trigger
- Full granularity calorimetry information
- Upgrade part of the muon systems, fast trigger

**Phase 2 Inner Tracker:** current ID will become inefficient due to radiation damage; too high occupancy in TRT; high granularity ( $\sim 4x$  better) required to cope with high pileup ( $\sim$  up to 200)



SLIGHTLY OBSOLETE